Human Molecular Genetics, 2016, Vol. 25, No. 6 1043–1058

doi: 10.1093/hmg/ddv513
Advance Access Publication Date: 17 December 2015
Original Article

ORIGINAL ARTICLE

AMPK activation protects from neuronal dysfunction and vulnerability across nematode, cellular and mouse models of Huntington's disease

Rafael P. Vázquez-Manrique[1,2,3,*], Francesca Farina[1,2], Karine Cambon[4,5], María Dolores Sequedo[3], Alex J. Parker[6,7], José María Millán[3], Andreas Weiss[8], Nicole Déglon[4,9] and Christian Neri[1,2,*]

[1]CNRS, UMR 8256, Laboratory of Neuronal Cell Biology and Pathology, Paris, France, [2]Sorbonnes Universités, University Pierre and Marie Curie (UPMC) Univ Paris 06, Paris, France, [3]Molecular, Cellular and Genomic Biomedicine Research Group, Health Research Institute-La Fe and CIBER de Enfermedades Raras (CIBERER), Valencia, Spain, [4]Commissariat à l'Energie Atomique et aux Energies Alternatives (CEA), Département des Sciences du Vivant (DSV), Institut d'Imagerie Biomédicale (I2BM), MIRCen, [5]Centre National de la Recherche Scientifique (CNRS), Université Paris-Sud, Université Paris-Saclay, UMR 9199, Neurodegenerative Diseases Laboratory, F-92260 Fontenay-aux-Roses, France, [6]CRCHUM, Montréal, Canada, [7]Department de Neurosciences, Faculté de médecine, Université de Montréal, Montréal, Canada, [8]Evotec AG, Manfred Eigen Campus, Hamburg, Germany and [9]Department of Clinical Neurosciences (DNC), Lausanne University Hospital (CHUV), Lausanne, Switzerland

*To whom correspondence should be addressed at: Centre National de la Recherche Scientifique, UMR 8256, Laboratory of Neuronal Cell Biology and Pathology, Paris, France; Sorbonnes Universités, University Pierre and Marie Curie (UPMC) Univ Paris 06, Paris, France. Tel: +33 144276045; Fax: +33 144275140; Email: christian.neri@inserm.fr (C.N.); rafael_vazquez@iislafe.es (R.P.V.-M.)

Abstract

The adenosine monophosphate activated kinase protein (AMPK) is an evolutionary-conserved protein important for cell survival and organismal longevity through the modulation of energy homeostasis. Several studies suggested that AMPK activation may improve energy metabolism and protein clearance in the brains of patients with vascular injury or neurodegenerative disease. However, in Huntington's disease (HD), AMPK may be activated in the striatum of HD mice at a late, post-symptomatic phase of the disease, and high-dose regiments of the AMPK activator 5-aminoimidazole-4-carboxamide ribonucleotide may worsen neuropathological and behavioural phenotypes. Here, we revisited the role of AMPK in HD using models that recapitulate the early features of the disease, including *Caenorhabditis elegans* neuron dysfunction before cell death and mouse striatal cell vulnerability. Genetic and pharmacological manipulation of *aak*-2/AMPKα shows that AMPK activation protects *C. elegans* neurons from the dysfunction induced by human exon-1 huntingtin (Htt) expression, in a *daf-16*/forkhead box O-dependent manner. Similarly, AMPK activation using genetic manipulation and low-dose metformin treatment protects mouse striatal cells expressing full-length mutant Htt (mHtt), counteracting their vulnerability to stress, with reduction of soluble mHtt levels by metformin and compensation of cytotoxicity by AMPKα1. Furthermore, AMPK protection is active in the

Received: September 19, 2015. **Revised and Accepted:** December 10, 2015

mouse brain as delivery of gain-of-function AMPK-γ1 to mouse striata slows down the neurodegenerative effects of mHtt. Collectively, these data highlight the importance of considering the dynamic of HD for assessing the therapeutic potential of stress-response targets in the disease. We postulate that AMPK activation is a compensatory response and valid approach for protecting dysfunctional and vulnerable neurons in HD.

Introduction

Adenosine monophosphate activated kinase protein (AMPK) is an obligate heterotrimeric enzyme that is composed of AMPKα (catalytic core), AMPKβ and AMPKγ (regulatory units). AMPK is central to the regulation of energy homeostasis and phosphorylates a wide range of proteins, in response to metabolic changes, mostly ATP fluctuations, through allosteric binding of AMP or ADP to AMPKγ and/or phosphorylation of the α-subunit. After activation, AMPK phosphorylates a range of targets to inhibit catabolic pathways and to activate anabolic pathways to restore ATP homeostasis (1,2). However, AMPK is also able to respond by phosphorylation of different targets to a range of stress conditions to restore homeostatic balance of energy levels. For instance, AMPK can promote initiation of autophagy (2,3) through inhibition of mammalian target of rapamycin (mTOR) (4) or via phosphorylation of the forkhead box O 3a (FOXO3a) (5) under conditions of low levels of ATP or stress of different kinds.

The transcription factor FOXO, a member of the FOX (forkhead box) family of proteins, has different isoforms in mammals, although only one gene represents this family in *Caenorhabditis elegans*, *daf-16*. This protein is a downstream player of the insulin signalling pathway in *C. elegans* and mammals and a well-known master regulator of lifespan that interplays upstream and downstream to the AMPK function across living organisms. AMPK also operates in cross-talk with other members of the AMPK-like family. For instance, the liver kinase B1 (LKB1) is a primary upstream kinase of AMPK and it regulates polarity and also is a tumour suppressor (reviewed in 6). Moreover, LKB1 is the kinase responsible for AMPK phosphorylation in response to the drug metformin (7). Aside from the interaction with mTOR and FOXO3a, AMPK is able to regulate several physiological events in cells, by signalling through a large number of downstream targets. For instance, AMPK can activate PGC-1α, through the modulation of NAD^+/NADH ratios and subsequent activation of sirtuin 1 (SIRT1), which in turn induces mitochondrial biogenesis (reviewed in 8). AMPK can also phosphorylate Unc-51 like autophagy activating kinase 1 to promote mitophagy (9). In addition to modulating energy levels and stress response, AMPK is able to respond to a range of drugs. For example metformin, an indirect AMPK activator (10), is a widely prescribed drug to patients with type II diabetes and has positive effects to prevent conditions such as cancer (reviewed in 11) or kidney disease (reviewed in 12). As indicated by studies in *C. elegans*, where AMPKα, the catalytic core of AMPK, is encoded by *aak-1* and *aak-2*, *aak-2*/AMPKα is involved in lifespan extension (13–15). On the whole, AMPK is considered to be a master regulator of healthspan (2,16–18) and lifespan (13–15).

In the brain, AMPK activation may have several protective effects against anxiety-like behaviour (19) and ischaemia (20,21), which may involve activation of autophagy. In Alzheimer's disease (AD), the situation is controversial. While AMPK has been shown to alleviate phenotypes associated with AD by reducing oxidative stress, slowing-down the formation of amyloid plaques and promoting the removal of β-amyloid peptides by autophagy (15,22,23), other reports have suggested that it is AMPK inhibition that may be protective (24), suggesting a complex picture in which gender effects may be involved as activation of AMPK may increase memory dysfunction in male AD mice, but may be protective in female AD mice (25). In Huntington's disease (HD), metformin, an antiglycemic drug and a well-known AMPK activator, may protect from the disease in a transgenic mouse model (R6/2) of HD (26), suggesting that AMPK activation has neuroprotective effects with therapeutic potential in HD. However, Ju *et al.* (27) have suggested that AMPK may be activated in the striatum of HD mice at a late stage of the disease and that chronic exposure to high-dose regiments of the AMPK activator 5-aminoimidazole-4-carboxamide ribonucleotide may worsen neuropathological and behavioural phenotypes. Ju *et al.* also suggested that AMPK may work downstream of oxidative stress to mediate neuronal atrophy in HD (28).

Here, we hypothesized that AMPK activation may be primarily protective during the early phases of the pathogenic process in HD, before cell death and during the early phases of neuronal decline (neuronal dysfunction without advanced degeneration). Using a *C. elegans* model of neuronal dysfunction in HD (29), we observed that metformin strongly reduces neuronal dysfunction caused by polyQ-expanded human exon-1 huntingtin (Htt) at the young adult stage. We also show that ablation of *aak-2*/AMPKα aggravates neuronal dysfunction in these animals in a cell autonomous and *daf-16*/FOXO-dependent manner. Genetic and chemical manipulation of AMPK in striatal cells derived from the HdhQ111 knock-in mouse model of HD (30) recapitulates the observations in polyQ nematodes. Furthermore, overexpressing AMPK counteracted the induction of neurodegeneration by lentivirus-mediated mutant Htt (mHtt) expression in mice striata, providing a proof-of-concept that AMPK can protect from mHtt cytotoxicity in the context of a living brain. Collectively, our data reveal that AMPK activation, which has anti-ageing effects in normal conditions, also has neuroprotective effects as the pathogenic process develops in HD, providing a rationale for further evaluation of small molecule activators of AMPK in the disease.

Results

aak-2/AMPK is protective in a *C. elegans* model of neuronal dysfunction in HD

The function of AMPK has been linked to lifespan and health span increase in nematodes and mice (13,31–33). Hence, we sought to test whether this enzyme may allow neurons to compensate for the stress and dysfunction that may be produced by mHtt expression during the early phases of HD pathology. To this end, we introduced a loss-of-function (LOF) allele of *aak-2*, *namely aak-2(ok524)*, one of the two worm homologues of AMPKα1 (13) into a nematode model of neuronal dysfunction in HD. While we initially attempt to do the cross in nematodes with stable co-expression of human exon-1 Htt and YFP (29), double mutants could not be isolated likely because the Htt transgene is inserted near to the *aak-2* locus. We, then, turned to single-transgenic animals. These animals bear a transgene that expresses the first exon of human Htt, with expanded (128Q) or normal (19Q) polyglutamines (polyQ) fused to green fluorescent protein (GFP) in touch receptor neurons (34). In 128Q nematodes, response to

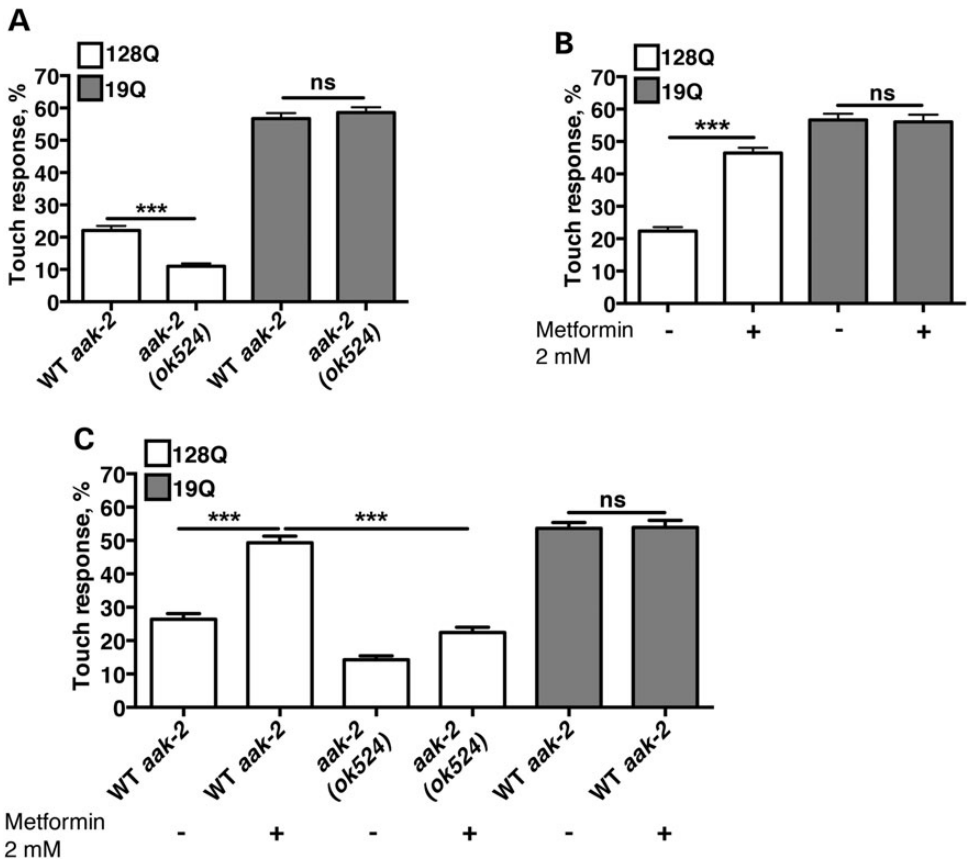

Figure 1. *aak-2*/AMPKα is neuroprotective in 128Q worms. (**A**) Ablation of the *aak-2* gene results in enhancement of the touch phenotype in 128Q worms. (**B**) Metformin alleviates the touch phenotype of 128Q animals, without affecting the behaviour of 19Q worms. (**C**) Metformin rescue of the worms depends mostly on the presence of the *aak-2* gene. In all panels, values are mean ± SEM ($N = 3$ with a total of at least 100 animals tested per condition). ANOVA tests, with Tukey *post hoc* analysis. Ns: not significant. $^{***}P < 0.001$.

light touch is strongly impaired compared with19Q nematodes (34) (Fig. 1A). The *aak-2* LOF further reduces touch response in 128Q animals without affecting touch response in 19Q animals (Fig. 1A). This effect was unrelated with a change of transgene expression (Supplementary Material, Fig. S1). This indicated that *aak-2* has neuroprotective effects in 128Q nematodes.

Next, we sought to examine whether AMPK activators might be protective in 128Q nematodes. It has been suggested that metformin partially inhibits complex I of the mitochondrial electron transport chain, which in turns increases the ADP/ATP ratio and activates AMPK (35). Here, we tested whether metformin might be able to ameliorate touch response impairment in 128Q nematodes. Metformin treatment at low doses (2 mM in the media, which may translate in a concentration that is 100 times less in the animals than in the media) strongly enhanced touch response of 128Q animals with no effect detected in 19Q animals (Fig. 1B). Additionally, compared with 128Q nematodes, 128Q; *aak-2(ok524)* nematodes show a loss of response to the positive effect of metformin treatment (Fig. 1C), suggesting that metformin protection is mostly dependent on *aak*-2/AMPK and may engage AMPKα activation.

aak-2/AMPK protects 128Q nematode neurons in a cell autonomous and *daf*-16/FOXO manner

We previously showed that DAF-16/FOXO, a master regulator of lifespan and healthspan in several organisms including *C. elegans* and mammals, has strong protective effects in *C. elegans* and mammalian-cell models of HD pathogenesis (29,36,37). Interestingly, FOXO factors are well-described effectors of AMPK under conditions of fasting, to promote lifespan extension in nematodes (38). Other studies have shown that both *aak-2* and *daf-16* are downstream in-parallel effectors in regulating lifespan through insulin signalling (31), suggesting that the AMPK-FOXO pathway may have a complex signalling loop. Given this, we sought to investigate whether the neuroprotection exerted by *aak-2*/AMPK in 128Q nematode neurons may be dependent on *daf-16*/FOXO. To this end, we crossed exon-1 Htt nematodes to a *daf-16* LOF mutant, *daf-16(mu86)*. The *daf-16* LOF strongly aggravated (50%) the loss of touch response in 128Q nematodes (Fig. 2), as expected and previously reported (36). Touch response in 128Q;*daf-16* nematodes is comparable to that of 128Q;*aak-2* nematodes (Fig. 2) and double mutants 128Q;*aak-2*;*daf-16* do not show an additive effect. This could suggest that *aak-2* and *daf-16* may operate in the same pathway to promote the touch receptor neuron function. However, touch responses in single and double mutants is very low, ~10–12%, and we cannot rule out the possibility that touch response can no longer be decreased and a synergistic effect could be missed in 128Q;*aak-2*;*daf-16* animals. To gain more insight into this question, we performed cell-specific rescue of *aak-2* and *daf-16*, into the single and double mutants. To this end, we produced transgenic nematodes carrying extrachromosomal arrays expressing a cDNA for *aak-2* or *daf-16* in touch receptor neurons. On the one hand, we introduced

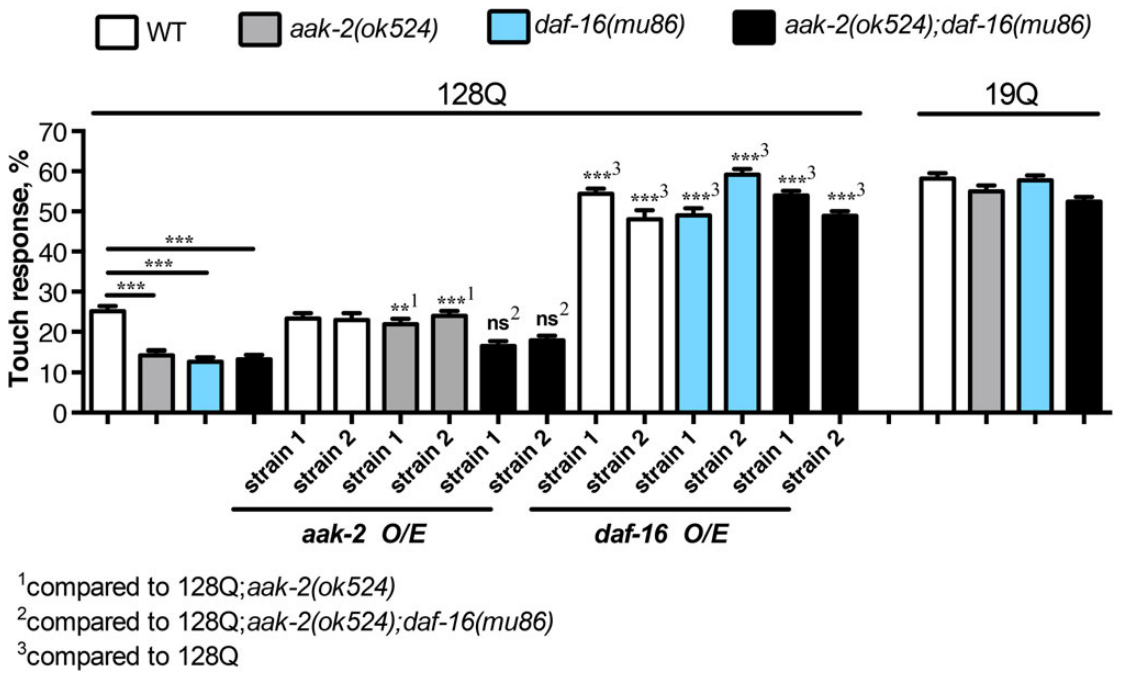

Figure 2. *aak-2* requires *daf-16* for neuroprotection in a tissue-specific-dependent manner. The deletion of both *daf-16* and *aak-2* induce a similar enhancement of the touch phenotype. Combining both mutations do not show a synergistic effect, neither an additive effect, suggesting that both genes induce neuroprotecttion though the same pathway. Rescuing *aak-2* and *daf-16* in mechanosensory neurons rescues the touch phenotype at different levels. Rescue of the touch phenotype by *aak-2* overexpression requires *daf-16*, further suggesting that both work in the same signalling pathway. Values are mean ± SEM ($N = 3$ with a total of at least 100 animals tested per condition). ANOVA tests, with Tukey *post hoc* analysis were used. ns: not significant. $^{**}P < 0.01$ and $^{***}P < 0.001$.

arrays expressing *aak-2* into the 128Q, 128Q;*aak-2* and 128Q;*aak-2*; *daf-16* animals. On the other hand, we introduced arrays expressing *daf-16* into 128Q, 128Q; *daf-16* and 128Q;*aak-2*;*daf-16* animals. We generated and analysed two independent strains per array (Fig. 2). Overexpression of *aak-2* or *daf-16* rescued neuronal dysfunction of 128Q animals in a cell-autonomous manner (Fig. 2). However, the level of rescue differs substantially between genotypes. The *daf-16* expression rescues the touch phenotype of all three strains into which it was introduced (128Q, 128Q;*daf-16* and 128Q;*aak-2*;*daf-16*) to levels comparable with 19Q nematodes (Fig. 2). This suggests that *daf-16* expression in touch receptor neurons is sufficient to restore a normal activity of these cells. This also suggests that *daf-16* acts downstream of *aak-2* since *daf-16* does not need *aak-2* to alleviate the touch response phenotype induced by polyQ-expanded Htt expression. In contrast, *aak-2* expression alleviates the touch response of 128Q;*aak-2* animals to the same level of 128Q, but has no effect in either 128Q or 128Q; *aak-2*;*daf-16* animals (Fig. 2). Why expression of *aak-2* cannot raise the mechanosensory response of 128Q animals to levels comparable with 19Q animals, as *daf-16* does? This can be attributed to AMPK operating as an obligate heterotrimer (AMPKα, AMPKβ and AMPK γ) in a range of species, from yeast to humans. Therefore, re-introducing *aak-2*/AMPKα alone cannot raise AMPK function above endogenous levels, since *aak-2* would need the other two components of the enzyme (AMPKβ and AMPKγ) in equimolar amounts, to be able to phosphorylate its substrates, including DAF-16. Nonetheless, failing of *aak-2* to rescue the touch phenotype of 128Q;*aak-2*;*daf-16* animals means that *daf-16* is epistatic over *aak-2* and so *daf-16* may act directly downstream of *aak-2* to protect neurons from 128Q cytotoxicity.

We previously showed that increasing the activity of sirtuin *sir-2.1*/SIRT1 protects 128Q nematodes from neuronal dysfunction in a *daf-16*-dependent manner (36,37). Subsequent studies showed that SIRT1 has neuroprotective effects in mouse models of HD (39,40). Given that SIRT1 may activate AMPK to ameliorate age-related diseases (41), we tested whether *sir-2.1*/SIRT1 protection may be dependent AMPK in 128Q nematodes. To this end, we introduced a null allele of *aak-2* in a strain of 128Q animals that has increased *sir-2.1*/SIRT1 dosage and that is devoid of background mutations with life extension effects (42). The protection from neuronal function elicited by increased *sir-2.1*/SIRT1 dosage in 128Q animals was completely abolished by *aak-2* LOF (Supplementary Material, Fig. S2), suggesting that sirtuin protection may be dependent on AMPK activity in HD neurons. Thus, SIRT1 may engage FOXO (36,37) and AMPK (this study)-dependent mechanisms to compensate for the neuronal cytotoxicity of mHTT species.

AMPKα is protective in mouse striatal cells derived from knock-in HD mice

To test whether the neuroprotective role of AMPKα observed in 128Q nematodes is conserved in a mammalian model of HD, we manipulated the activity of AMPKα in striatal cells derived from the HdhQ111 knock-in mouse model of HD (30). Striatal cells expressing mHtt (109Q/109Q) are abnormally susceptible to cell death as induced by serum deprivation (30), a phenotype that is suitable for identifying modifiers of cell vulnerability in HD (30,43). The analysis of the expression levels of the two AMPK catalytic isoforms present in mammals, AMPKα1 and AMPKα2, by quantitative real-time polymerase chain reaction (qRT-PCR) shows that both types of mRNAs are present in striatal cells derived from the HdhQ111 mice (Fig. 3A). This analysis primarily suggested that AMPKα1 mRNA levels are higher in 109Q/109Q cells than those in 7Q/7Q cells whereas AMPKα2 mRNA levels were lower in 109Q/109Q cells than those in 7Q/7Q

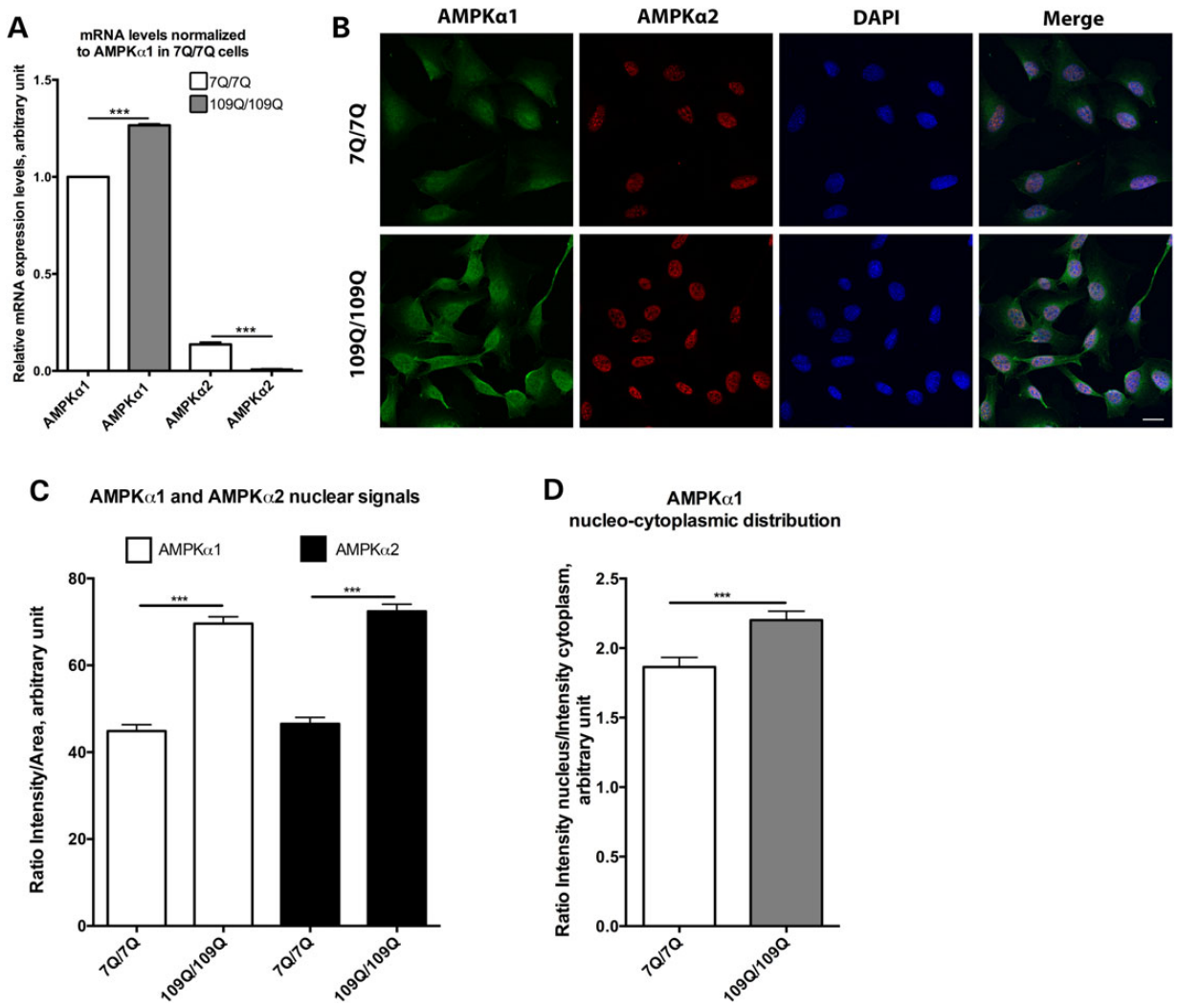

Figure 3. Nucleo-cytoplasmic expression of AMPKα1 and AMPKα2 in 7Q/7Q and 109Q/109Q mouse striatal cells. (**A**) RT-PCR analysis of the expression of AMPKα subunits shows that AMPKα1 mRNA levels are higher in 109Q/109Q cells versus 7Q/7Q cells and that AMPKα2 mRNA levels are lower in 109Q/109Q cells versus 7Q/7Q cells. Values are mean ± SD ($N = 3$ in triplicate). ***$P < 0.001$. (**B**) Representative images of antibody staining of both subunits showing that AMPKα1 and AMPKα2 have variable nucleo-cytoplasmic distributions across 7Q/7Q and 109Q/109Q cells. Scale bar is 20 μM. (**C**) Quantification of nuclear signal intensities for AMPKα1 and AMPKα2 showing that there is more AMPKα1 in 109Q/109Q cells compared with 7Q/7Q cells, which is also observed for AMPKα2. Values are mean ± SEM ($N = 3$ for a total of at least 90 cells tested per condition). ***$P < 0.001$. (**D**) Quantification of nucleo-cytoplasmic distribution for AMPKα1 showing that there is more AMPKα1 in the nucleus of 7Q/7Q cells, which is more pronounced in 109Q/109Q cells. Values are mean ± SEM ($N = 3$ for a total of at least 90 cells). ***$P < 0.001$. Statistics were performed using *t* tests in all panels.

cells (Fig. 3A). Confocal analysis shows that AMPKα1 is localized in the cytoplasm and nucleus of 7Q/7Q and 109Q/109Q cells (Fig. 3B) and that there is more AMPKα1 expression in 109Q/109Q versus 7Q/7Q cells with AMPKα1 proteins being primarily detected in the nucleus (Fig. 3C and D), which corroborates the trend detected at the mRNA level. Consistently with previous studies (44), AMPKα2 is mostly nuclear in mouse striatal cells (Fig. 3B). Confocal analysis also shows that there is more AMPKα2 in 109Q/109Q cells compared with 7Q/7Q cells (Fig. 3C). This contrasts with the trend observed at the mRNA level, suggesting that AMPKα2 proteins are prone to stabilization in 109Q/109Q and 7Q/7Q cells.

It has been suggested that overactivation and nuclear translocation of AMPKα1 may exacerbate cell death during the late phases of the pathogenic process in HD as inferred from the study of HD post-mortem brains and mouse models of HD, such as symptomatic R6/2 mice (12 weeks) probably due to oxidative stress (27,28). It has also been suggested that AMPK phosphorylation and activation is associated to cytotoxicity in striatal cell lines derived from HdhQ111 knock-in mouse (27,28). However, when we add the AMPK activator metformin (2 mM) to these cells (109Q/109Q cells), we observed an increase of AMPKα-phosphorylated levels in the nucleus and cytoplasm of 7Q/7Q and 109Q/109Q cells, with a trend towards a slightly stronger effect in the cytoplasm of 109Q/109Q cells (Fig. 4A and B). We also observed that metformin treatment reduced the susceptibility to cell death induced by serum deprivation in mHtt striatal cells (Fig. 5A), a phenotype previously shown to be dependent on mHtt expression (37), with no effect detected in normal Htt striatal cells (Fig. 5A), which is accompanied by increased phosphorylation of AMPKα (Fig. 5A). Moreover, while RNAi silencing of AMPKα2 does not change the mortality rate of serum-deprivated 109Q/109Q cells (data not shown), siRNA against the more abundant form AMPKα1 strongly increased the mortality of 109Q/109Q cells with no effect detected in 7Q/7Q cells. This suggests that AMPKα1 has a protective role in cells expressing

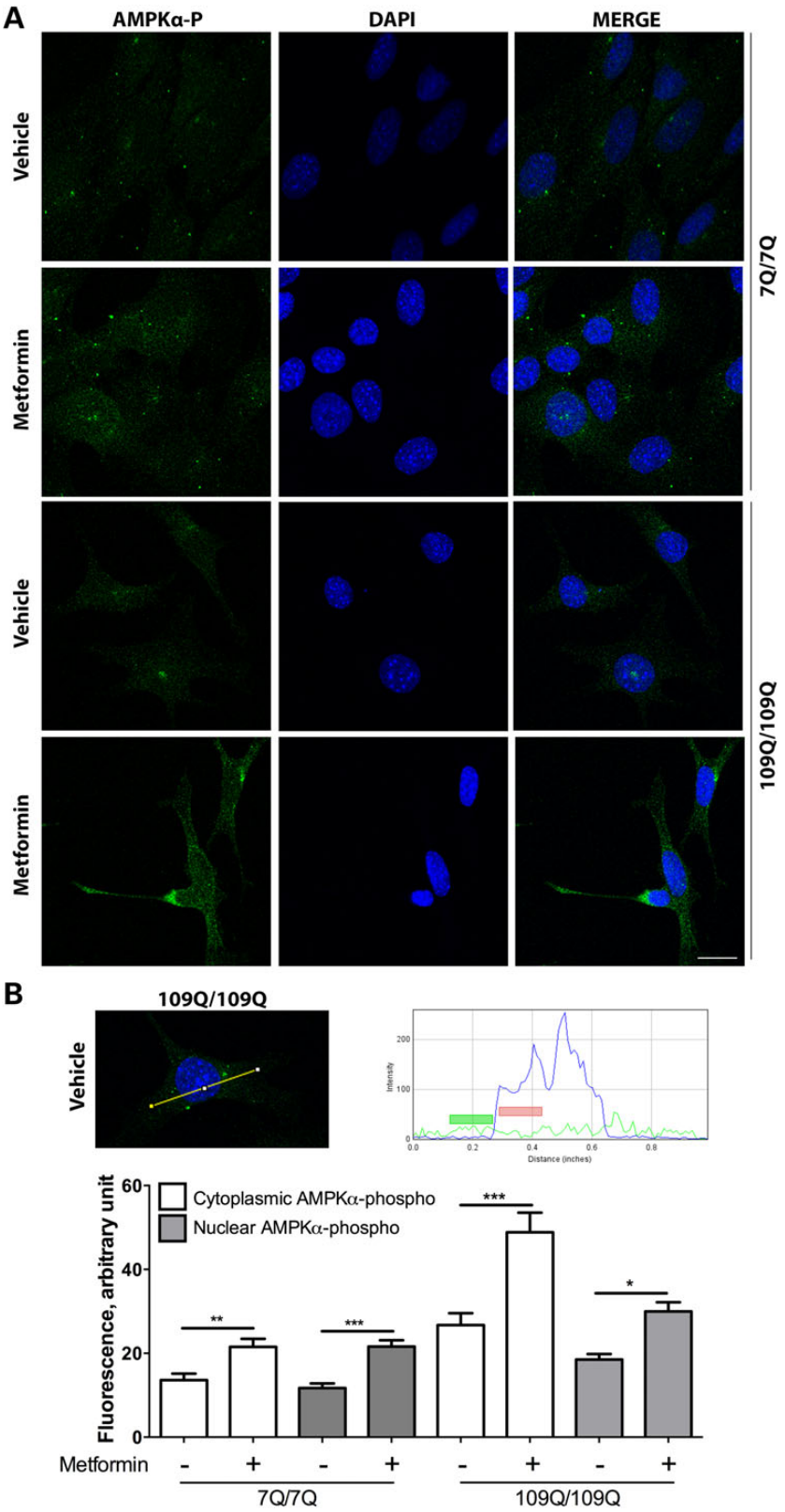

Figure 4. Nucleo-cytoplasmic expression of AMPKα-phosphorylated in 7Q/7Q and 109Q/109Q mouse striatal cells. (**A**) Representative confocal images illustrating that AMPKα-phosphorylated is evenly distributed in the nucleus and cytoplasm in 7Q/7Q and 109Q/109Q cells. Scale bar is 20 µm. (**B**) The upper two panels show an example of the AMPKα-phosphorylated signal along a line (yellow) that crosses the cytoplasm and nucleus. The blue curve shows DAPI staining, pointing out the region covered by the nuclei, and the green line shows fluorescent due to AMPKα-phosphorylated staining. Colour boxes indicate the area used for the quantification of AMPKα-phosphorylated signals on either side of the nuclear membrane. The lower panel shows the levels of AMPKα-phosphorylated signals, with increase of the signal in both the cytoplasmic and nuclear compartment induced by metformin treatment of 7Q/7Q and 109Q/109Q cells. Values are mean ± SD (N = 3 for a total of at least 50 cells/condition). ANOVA tests, with Tukey *post hoc* analysis for each genotype, were used. $^{*}P < 0.05$, $^{**}P < 0.01$ and $^{***}P < 0.001$.

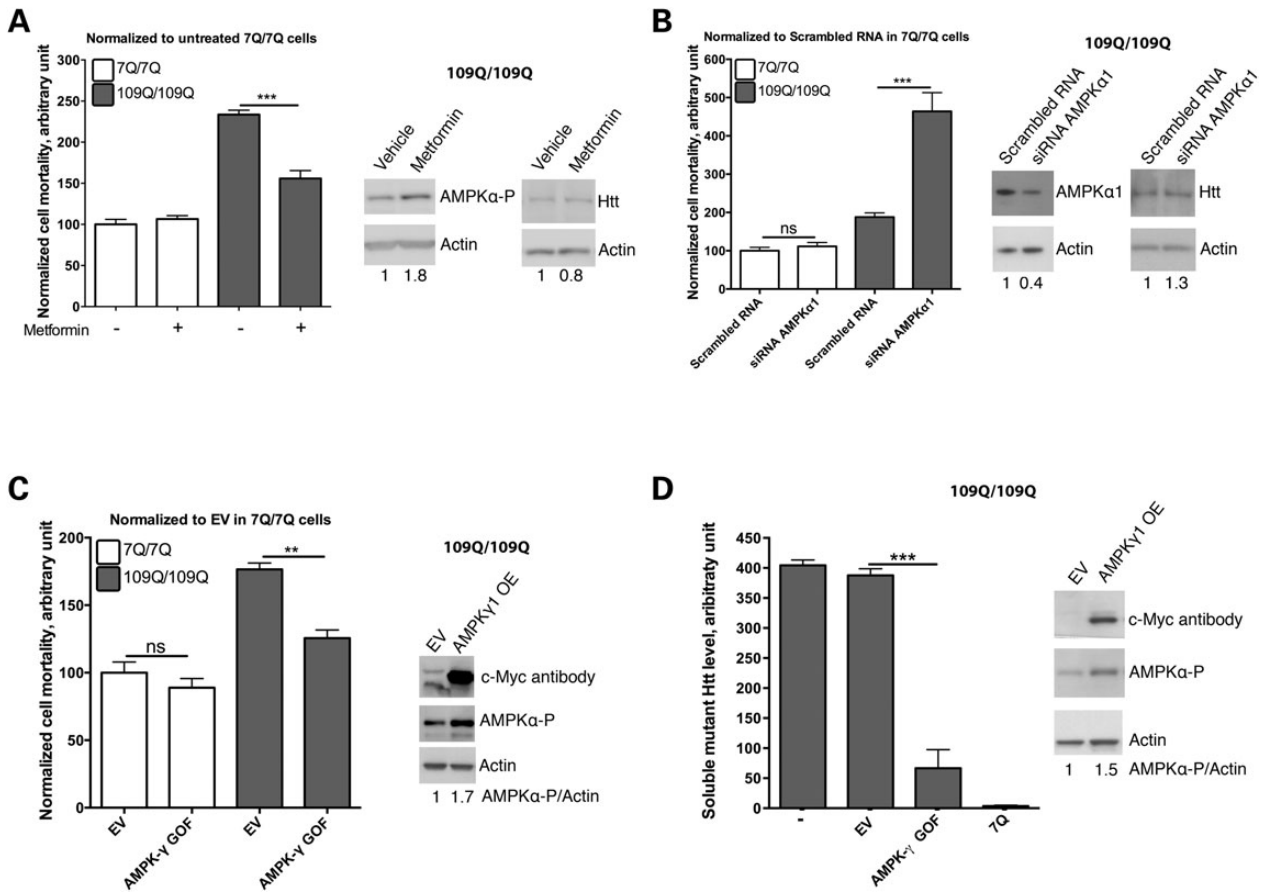

Figure 5. AMPK has a protective function in and *in vitro* model of HD. (**A**) Growing striatal cells in metformin 2 mM reduces mortality induced by serum deprivation in 109Q/109Q mouse striatal cells (***$P < 0.001$, $N = 3$). The right panel shows representative western blots to show that AMPKγ1GOF induces phosphorylation of AMPKα in striatal cells. The levels of Htt do not change. (**B**) Silencing AMPKα1 by RNAi in 109Q/109Q mouse striatal cells enhances cell mortality in response to serum deprivation with no effect detected in 7Q/7Q cells (***$P < 0.001$; ns: not significant; $N = 3$). The right panel shows representative western blots in which AMPKα1 siRNAs reduce AMPKα1 protein levels ($N = 3$, mean ± SD = 0.4 ± 0.1, $P = 0.018$) with no change detected in the level of Htt ($N = 3$, mean ± SD = 1.1 ± 0.5, $P = 0.71$). (**C**) Overexpression of an over-activated form of AMPKγ1, AMPKγ1GOF, reduces mortality of 109Q/109Q cells in response to serum deprivation (**$P < 0.005$, $N = 3$). The right panel shows representative western blots in which AMPKγ1GOF expression increases AMPKγ1 protein levels (as detected using a c-Myc tag), phosphorylated AMPKα1 levels ($N = 3$, mean ± SD = 1.6 ± 0.1, $P = 0.027$). The effect on Htt levels is addressed in (**D**). (D) Overexpression of the over-activated form of AMPKγ1 induces clearance of misfolded mHtt (***$P < 0.001$, $N = 3$). The right panel shows representative western blots in which AMPKγ1GOF increases AMPKγ1 levels (as detected using a c-Myc tag), and phosphorylated AMPKα levels ($N = 4$, mean ± SD = 1.7 ± 0.4, $P = 0.021$). In all panels: ns: not significant.

mHtt (Fig. 5B). Next, we tested for the effect of AMPK activation in these cells. To this end, we introduced in these cells a gain of function form of AMPKγ1, the regulatory subunit of the enzyme that induces a constitutively active state in the catalytic subunit AMPKα. We elected to manipulate AMPKγ1 levels as a way to test for the effects of different types of AMPK subunits on AMPK activation and cell survival. Overexpression of AMPKγ1 gain of function (AMPKγ1GOF) induces phosphorylation of AMPKα paralleled with an increase of the survival of mouse striatal cells expressing mHtt with no effect detected in mouse striatal cells expressing normal Htt (Fig. 5C). These effects occur without perturbing the expression of mHtt (Fig. 5C). For all experiments based on using striatal cells from HD mice, it is noticeable that we used low passage (P9–P11) mouse striatal cells, which is an important consideration since the mouse striatal cell lines expressing mHtt tend to lose their cell vulnerability phenotype at higher passages. Our results thus suggest that changes in the brains from HD patients, at the time of death, and in R6/2 mice, at an advanced stage of pathology (12 weeks), in terms of AMPKα activity and outcome on cell survival may greatly differ from changes observed in models that recapitulate an earlier or milder phase of cytotoxicity in HD such as mouse striatal cells derived from HdhQ111 knock-in mice.

Collectively, these data suggest that raising AMPK activity protects striatal cells from the vulnerability to stress that may be induced by mHtt expression in HD.

Raising AMPK activity reduces the amount of soluble mHTT in mouse striatal cells derived from HdhQ111 mice

AMPK can promote protein clearance in response to cellular stress induced by nutrient deprivation, through inhibition of mTOR (45). Additionally, AMPK can activate autophagy and protein clearance in muscle cells through activation of the longevity-promoting factor FOXO3a (46). AMPK can also modulate the function of the proteasome under specific metabolic conditions such as nutrient deprivation (3). Therefore, we tested whether alleviation of stress vulnerability of 109Q/109Q striatal cells by AMPK activation (Fig. 5A–C) might be associated to a reduction of mHTT load. To this end, we assayed 109Q/109Q striatal cells in which we had over-expressed AMPKγ1GOF using an ultrasensitive

method that relies on antibody staining and Förster resonance energy transfer for the specific quantification of soluble mHTT levels (47). Interestingly, 109Q/109Q cells transfected with AMPKγ1-GOF show a drastic reduction of soluble mHtt levels (Fig. 5D), suggesting that raising AMPK activity protects mouse striatal cells from cell vulnerability by reducing soluble mHtt levels.

Expression of AMPKγ1GOF protects the mouse striatum from mutant Htt protein load

Our results from the *C. elegans* and mouse striatal cell models of HD pathogenesis consistently suggest that AMPK has neuroprotective effects against the early phases (neuronal dysfunction) or features (cell vulnerability) of mHtt cytotoxicity. Next, we tested whether AMPK protection may also occur *in vivo* in the mouse brain. To this end, we used a model in which expression of N-terminal Htt in the striatum using lentiviral vectors produce neurodegeneration at 6–7 weeks. This murine model may be considered a mild model of proteotoxic stress in HD since these animals are born free of mHtt and since lentiviral vectors elicit a moderate level of mHtt expression. We co-injected C57Bl/6J mice bilaterally (i.e. in each of the striatum hemispheres) with lentiviral vectors expressing Htt171-82Q plus saline (left hemisphere: control) and Htt171-82Q +AMPKγ1GOF (right hemisphere: test) (Fig. 6A). Seven weeks after injection, animals were sacrificed and DARPP32 (Dopamine- and cAMP-regulated phosphoprotein, a neuronal marker well expressed by the medium spiny neurons of the striatum which are particularly vulnerable in HD) and ubiquitin (UBI) staining were used to monitor the level of striatal pathology (Fig. 6A). The lesion size of the animals over-expressing AMPKγ1GOF is significantly reduced by 27% compared with controls (Fig. 6B), suggesting that AMPK activation can slow-down the neurodegenerative process induced by mHTT expression in the brain. In contrast, the total number of UBI positive aggregates shows no significant change (Fig. 6B), suggesting that AMPK activation protects through mechanisms that do not involve removal of inclusion bodies of mHTT.

Discussion

Premanifest or early-stage symptoms of HD are increasingly accessible to the follow-up studies and, potentially, disease modification in human patients (48). At these stages of HD, cellular dysfunction and vulnerability may represent an important and targetable component of the disease compared with later stages of HD in which striatal cell loss is a prominent feature of the disease. It, thus, becomes essential to investigate the activity of HD targets in model systems that recapitulate the early and reversible components of the disease process such as neuron dysfunction before cell death and neuronal tissue vulnerability. We previously showed that activation of cell survival and longevity pathways such as the *sir-2.1* and *daf-16* pathway protects from such components of the pathogenic process in HD (29,36,37). Among these pathways, AMPK stands as a sensor of energy state and guardian of energy homeostasis that may protect the brain from insults such as stroke and neurodegenerative disease-associated proteins.

Like many other HD targets at the cross-roads of signalling pathways that are essential for cellular maintenance and cell survival, AMPK is part of a large network of highly interconnected genes that may change behaviour depending on the strength of the proteotoxic stress and stage of the pathogenic process in HD. In this context, it is important to understand what may be the consequence of activating or inhibiting such targets across several phases of the pathogenic process in HD. Additionally, the net outcome of manipulating a highly connected (hub gene) target is likely to reflect the balance between a series of protective effects on the one hand and a series of aggravating effects on the other hand, with each type of effects potentially engaging different neighbours and downstream targets. This balance is highly sensitive to the genetic and biological status of any one model in which the target is manipulated. Here, we used highly controlled models of HD pathogenesis (staged nematode strains, low-passage mouse striatal cells, calibrated delivery of Htt to mouse striata) to investigate the effects of manipulating AMPK activity on a cardinal component that may underlie the dynamic of HD, namely constitutive cell vulnerability, a cellular state that may promote the early dysfunction and demise of HD neurons and that may be associated to 'build-in deficiency' of stress response mechanisms such as those under the control of FOXO3a (29). Our genetic data suggest that AMPK primarily protects from such constitutive and early-stage features of the pathogenic process in HD, with capacity to reduce the ultimate level of neurodegeneration that is progressively induced by misfolded Htt expression. Noticeably, AMPKα1 levels are increased in mouse striatal cells expressing mHtt and AMPKα1 silencing aggravates the vulnerability of these cells to cell death induced by serum deprivation, suggesting that AMPKα1 has a compensatory and protective role in these cells.

Our findings contrast with data from Ju *et al.* who reported that the function of AMPK might be over-activated, paralleled by an AMPKα1 translocation to the nucleus, in symptomatic mouse models of HD and post-mortem HD brain tissues as a consequence of oxidative stress (27,28). These latter studies used models that recapitulate a fast developing, and rather advanced phase, of HD pathology (symptomatic R6/2 mice at 12 weeks) in mice or a late phase of the disease in human subjects (post-mortem HD brain). Their results contrast with the observation that giving metformin to a transgenic model of HD (R6/2) has been shown to increase the brain ratio of AMPKα-phosphorylated versus non-phosphorylated, an effect accompanied by an amelioration of some of the phenotypes associated with the disease (26). Here, we used models that recapitulate the early (neuronal dysfunction in young *C. elegans* adults), constitutive (cell vulnerability of mouse striatal cells) and progressive (neurodegeneration ultimately induced by lentiviral delivery in the mouse brain) phases of HD pathology to observe that AMPK activation is protective whether elicited by genetic or pharmacological means. We propose that AMPK activity may have diametrically opposing roles in HD depending on the biological phase of the pathogenic process in HD. Collectively, our data suggest a model in which the function of AMPK has a protective role in the early to intermediate phases of the pathogenic process in the disease, by inducing pro-survival pathways that prevent the cytotoxicity induced by soluble mHTT. Here, it is interesting to note that AMPK activators such as A769662 may be protective in mouse cell models of HD (C. Walter and H.P. Nguyen, personal communication) as we observed with the genetic and pharmacological activation of AMPK in our study. Collectively, the results in the two studies strongly emphasize AMPK and its activation as a valuable approach to preserve the capacity of striatal neurons to fight the consequences of mHTT toxicity and maintain homeostasis over the early, manageable phases of the pathogenic process in HD. As the organism ages or as cells are less capable of coping with proteotoxic stress and its consequences, AMPK might become more active by an overwhelming quantity of stress signals, and its activity may become lethal to the cell. Thus, careful attention should be given on how to test for the effects of

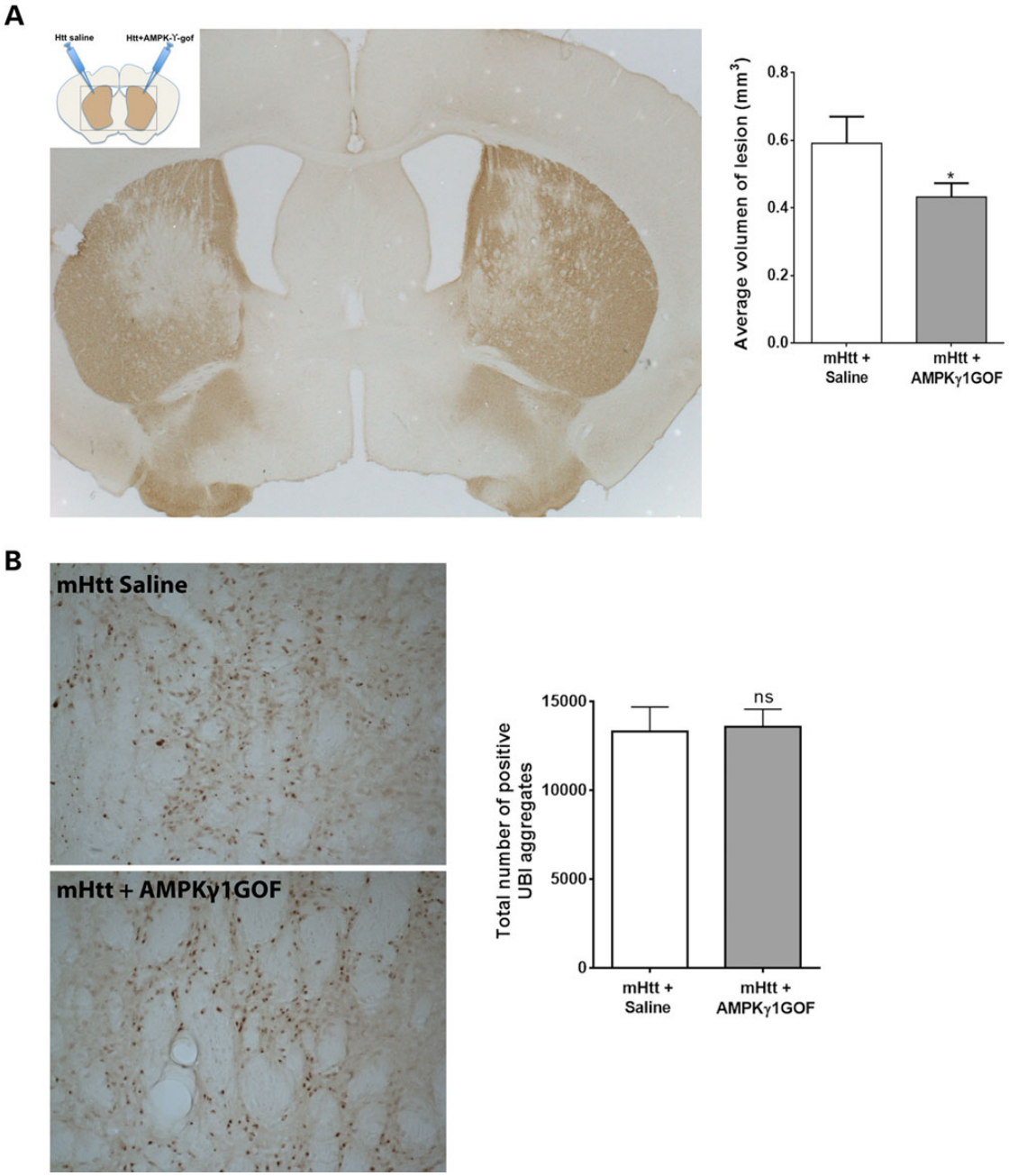

Figure 6. *In vivo* activation of AMPK rescues striatal cell degeneration in a mouse model of HD. (**A**) Diagram showing the treatment of both sides of the brains of mice with lentiviruses expressing the N-terminal fragment of mHtt [Htt171-82Q (Htt in the diagram)], or the AMPKγ1GOF. Below is shown a representative picture of DARPP32 staining of the sections of the brains of these mice, which highlights the area of the lesion caused by mutant Htt. The right panel shows the analysis of the volume of the lesion caused by mutant Htt, with overexpression of AMPKγ1GOF reducing cell death. Values are mean ± SEM. *$P < 0.05$ ($P = 0.03$, $N = 13$). (**B**) Representative pictures showing UBI staining and pointing out to inclusion bodies. The right panel shows the quantification of the number of UBI-positive aggregates. Values are mean ± SEM. The overexpression of AMPKγ1GOF does not change the number of inclusion bodies ($P = 0.87$, $N = 13$). Statistics use the Wilcoxon test for paired samples. ns: not significant.

AMPK modulation in pre-clinical studies aiming at the development of disease-modifying strategies.

Our data corroborate the important notion that longevity-promoting pathways such as the AMPK pathway may help neurons to deal with the proteotoxic stress that is chronically induced in neurodegenerative disease by misfolded protein expression such as mHtt (29,36,37,49), therefore sustaining the capacity for biological resilience to proteotoxic stress in HD cells and tissues. This is particularly important as biological resilience to proteotoxic stress may be impaired at an early stage of the HD process through the repression of the longevity-promoting and neuroprotective factor FOXO3 by increased Ryk signalling to the nucleus (29). Since AMPK may directly regulate FOXO3 protective activity (38), AMPK activators could provide a way to restore an efficient response of FOXO3 to proteotoxic stress in HD neurons. Additionally, our data in mouse striatal cells and in the mouse brain suggest that AMPK may induce mechanisms that clear the cell from toxic soluble species, without affecting the presence

of inclusion bodies. Examples of such apparent discrepancy are not rare in the literature, since it was shown early on that treatment with the caspase inhibitor Z-VAD-FMK increased the survival of mouse striatal cells transfected with mHtt, but failed to diminish nuclear and cytoplasmic inclusions. In the same way, another substance tested in HD models, Z-DEVD-FMK, significantly reduced inclusion bodies without increasing the survival of cells (50). Saudou *et al.* (51) showed that exposure to conditions that suppress the formation of inclusion bodies resulted in an increase in mHtt-induced cell death. Also, Zala *et al.* (52) reported that in rat primary striatal cultures infected with the same lentivirus encoding Htt171-82Q used in our study, the ciliary neurotrophic factor and brain-derived neurotrophic factor prevented neuronal degeneration while increasing the number of ubiquitinated nuclear inclusions. Finally, two more teams, Arrasate *et al.* and Mitra *et al.* (53,54) showed data strongly suggesting that inclusion bodies may be the consequence of a protective cellular mechanism.

Interestingly, our data suggest that AMPK activators such as metformin may protect from the early phases of the pathogenic process in HD. It has been shown that metformin may have anticancer (55) and antidiabetic (56) activities through AMPK-independent pathways. However, our experiments indicate that the rescue of neuronal impairment of the polyQ-expressing animals mediated by metformin is mostly dependent on the presence of *aak-2*/AMPKα. This strongly suggests that the AMPK function is required for a beneficial effect. Metformin has been shown to be able to extend health- and life-span in *C. elegans* (57) and in rodents (58) by mimicking caloric restriction. It has been proposed recently that lifespan extension in worms, treated with metformin, is mediated by inhibition of the microbial folate and methionine metabolism by this drug (59), an effect which is AMPK-dependent. Hence, it may be possible that metformin may be rescuing, at least partially, neuronal impairment of 128Q worms through mimicking caloric restriction. Another mechanism by which metformin may protect from mHTT cytotoxocity is the reduction of soluble mHTT levels, as revealed by our data in mouse striatal cells. As recently suggested in other studies of stress response drugs such as rapamycin (60) and latrepirdine (61), it is interesting to speculate that, besides a chronic exposure to AMPK activators that could have unwanted effects in the context of HD, intermittent, low-dose or pre-conditioning treatment with AMPK activators might constitute a safer though efficient way to activate AMPK activity and slow-down disease progression in early-stage HD. The purpose of our study was to generate a proof-of-concept that AMPK activation protects against the cytotoxic effects of mHTT *in vivo*, in the mouse brain. Future studies will test whether AMPK activators such as metformin and other compounds of potential interest for AMPK activation in neurons with proteotoxic stress (61–64), in the form of chronic, intermittent or pre-conditioning treatments, may have neuroprotective effects as the pathogenic process develops in transgenic and knock-in mouse models of HD. Here, it is important to note that since there is more AMPKα1 in 109Q/109Q mouse striatal cells, and since AMPKα1 silencing aggravates cell death in these cells whereas raising AMPK activity has opposite effect, AMPKα1 increase may represent a compensatory and protective response against mHtt expression and the early phases of the HD process.

In sum, our data suggest that AMPK activation represents a compensatory response and useful approach for protecting neurons that, in the caudate nucleus, are targeted by the early phases of the proteotoxic and cellular stress induced by mHTT expression in HD.

Materials and Methods

Nematode strains and culture

Nematodes were grown as described elsewhere (65). All strains were maintained and assayed at 20°C. Transgenic *C. elegans* nematodes stably expressing human Htt fused to GFP were previously described (29,34,37,66). Non-*dyf sir-2.1* over-expressing mutants were obtained from the laboratory of David Gems (42). The originating parent strain, LG100, has been described as having a Dyf (dye defective mutant) phenotype responsible, at least in part, regarding the pro-lifespan effects. Table 1 provides a detailed list of strains used in this study. All strains were outcrossed to wild-type background (Bristol N2) at least four times.

Genetic manipulation in *C. elegans*

To produce the constructs for the tissue-specific rescue experiments, we amplified the promoter of the *mec-3* gene using the following primers: forward RVM13 5′-GGGGACAAG TTTGTACA AAAAAGCAGGCTCCTGCAGGTACCCGGAGTAGTTG-3′ and reverse RVM14 5′-GGGGACAACTTTTGTATACAAAGTTGTAATGCGCGAAA TTGTGGCTAC TC-3′. We cloned this PCR product in pDONR-P1-P5r using the system Gateway (Invitrogen). We then amplified the cDNA of *aak-2*, using the following primers: forward RVM18 5′-GGGGACAACTTTGTATAC AAAAGTTGGAAAAATGTTTTCTCAT CAAGATCGAGA C-3′ and reverse RVM19 GGGGACCACTTTGTAC AAGAAAGCTGGGTATTAACGAGC CAGTGTTCCAATCAATG-3′. We amplified the cDNA of *daf-16* fused to GFP from a plasmid from the Driscoll Lab (Rutgers University, USA) using the following primers: primer RV177 5′-GGGGACAACTTTGTATACAAAAGTTGAAA ATGATGGAGATGCTGGTAG ATC-3′ and reverse RV178 5′-GGGGA CCACTTTGTACAAGAAAGCTGGGTATTATAG TTCATCCATGCCAT GTGTA-3′. Both PCR products, *aak-2* and *daf-16::GFP*, were cloned into pDONR-P5-P2 using Gateway. The *mec-3* promoter and each cDNA were assembled separately, using Gateway, within a destination vector that contains the transcription terminator from the *unc-54* gene, pHP2 (69).

For overexpression experiments, 20 ng/µl of the DNA containing the cDNA of interest was injected into worms, together with pPD118.33 (a plasmid encoding a pharyngeal-expressed GFP as a marker). pPD118.33 is a gift from A. Fire. DNA was injected at a total final DNA concentration of 120 ng/µl, using previously described methods (70). Several independent stable strains containing the transgenes were isolated, and at least two strains of each construct were analysed.

Behavioural assays in *C. elegans*

Touch test on posterior lateral microtubule neurons were performed by scoring for 10 touches on the tail of the animal for ~100 animals per genotype, as described elsewhere (66). We plotted mean values for responsiveness and analysis of variance (ANOVA) test, with Tukey's multiple comparison test, were used for statistical analysis.

Pharmacological assays in *C. elegans*

Synchronized L1 larvae were grown in the liquid culture as described previously (36) in the presence of metformin 2 mM (1,1-dimethylbiguanide hydrochloride, Sigma-Aldrich ref. D150959) or vehicle (dimethylsulfoxid, DMSO) as a control. Once they reached adulthood (48 h or so), animals were placed in empty NGM plates and allowed to rest for an hour. Animals were then assayed for response to light touch as described above.

Table 1 Names and genotypes of the *C. elegans* strains used in this study.

Strain[a]	Genotype	References
Bristol N2	Standard wild-type	(65)
CF1038	*daf-16(mu86)*-I	(67)
GA468[b]	*geIn3[sir-2.1; rol-6]*-I	(42)
RB754	*aak-2(ok524)*-X	(13)
ID161[c]	*igIs161[mec-3p::htt57-19Q::GFP; lin-15(+)]*-?	(66)
ID5	*igIs5[mec-3p::htt57-128Q::GFP; lin-15(+)]*-?	(66)
ID1400	*igIs161[mec-3p::htt57-19Q::GFP; lin-15(+)]*-?; *aak-2(ok524)*-X	This work
ID1401	*igIs5[mec-3p::htt57-128Q::GFP; lin-15(+)]*-?; *aak-2(ok524)*-X	This work
ID1402	*igIs161[mec-3p::htt57-19Q::GFP; lin-15(+)]*-?; *daf-16(mu86)*-I	This work
ID1403	*igIs5[mec-3p::htt57-128Q::GFP; lin-15(+)]*-?; *daf-16(mu86)*-I	This work
ID1404	*igIs161[mec-3p::htt57-19Q::GFP; lin-15(+)]*-?; *aak-2(ok524)*-X; *daf-16(mu86)*-I	This work
ID1405	*igIs5[mec-3p::htt57-128Q::GFP; lin-15(+)]*-?; *aak-2(ok524)*-X; *daf-16(mu86)*-I	This work
ID1406	*igIs5[mec-3p::htt57-128Q::GFP; lin-15(+)]*-?; *geIn3[sir-2.1; rol-6]*	This work
ID1407	*igIs5[mec-3p::htt57-128Q::GFP; lin-15(+)]*-?; *geIn3[sir-2.1; rol-6]; aak-2(ok524)*-X	This work
RVM100	*igIs5[mec-3p::htt57-128Q::GFP; lin-15(+)]*-?; *vltEx1[mec-3p::aak-2; myo-2::GFP]*	This work
RVM101	*igIs5[mec-3p::htt57-128Q::GFP; lin-15(+)]*-?; *vltEx2[mec-3p::aak-2; myo-2::GFP]*	This work
RVM102	*igIs5[mec-3p::htt57-128Q::GFP; lin-15(+)]*-?; *vltEx3[mec-3p::daf-16; myo-2::GFP]*	This work
RVM103	*igIs5[mec-3p::htt57-128Q::GFP; lin-15(+)]*-?; *vltEx4[mec-3p:: daf-16; myo-2::GFP]*	This work
RVM104	*igIs5[mec-3p::htt57-128Q::GFP; lin-15(+)]*-?; *aak-2(ok524)*-X; *vltEx5[mec-3p::aak-2; myo-2::GFP]*	This work
RVM105	*igIs5[mec-3p::htt57-128Q::GFP; lin-15(+)]*-?; *aak-2(ok524)*-X; *vltEx6[mec-3p::aak-2; myo-2::GFP]*	This work
RVM106	*igIs5[mec-3p::htt57-128Q::GFP; lin-15(+)]*-?; *daf-16(mu86)*-I; *vltEx7[mec-3p::daf-16; myo-2::GFP]*	This work
RVM107	*igIs5[mec-3p::htt57-128Q::GFP; lin-15(+)]*-?; *daf-16(mu86)*-I; *vltEx8[mec-3p:: daf-16; myo-2::GFP]*	This work
RVM108	*igIs5[mec-3p::htt57-128Q::GFP; lin-15(+)]*-?; *aak-2(ok524)*-X; *daf-16(mu86)*-I;*vltEx9[mec-3p::aak-2; myo-2::GFP]*	This work
RVM109	*igIs5[mec-3p::htt57-128Q::GFP; lin-15(+)]*-?; *aak-2(ok524)*-X; *daf-16(mu86)*-I;*vltEx10[mec-3p::aak-2; myo-2::GFP]*	This work
RVM110	*igIs5[mec-3p::htt57-128Q::GFP; lin-15(+)]*-?; *aak-2(ok524)*-X; *daf-16(mu86)*-I; *vltEx11[mec-3p:: daf-16; myo-2::GFP]*	This work
RVM111	*igIs5[mec-3p::htt57-128Q::GFP; lin-15(+)]*-?; *aak-2(ok524)*-X; *daf-16(mu86)*-I; *vltEx12[mec-3p:: daf-16; myo-2::GFP]*	This work

[a]All mutant strains were out-crossed to wild-type background (Bristol N2) at least four times. N2, CF1038, GA468 and RB754 were provided by the *Caenorhabditis* Genetics Centre (University of Minnesota, MN, USA).
[b]The GA468 strain contains a *sir-2.1* overexpressing transgene from the strain LG100 (68), but it does not contain the *dyf(?)* mutation present in LG100 (42).
[c]*htt57* refers to aminoacids 1–57 of human Htt.

Production of AMPKγ1GOF plasmid for use in cell or mouse testing

Mouse cDNA coding for the gamma1 subunit of AMPK tagged with c-Myc in a pDONR-221 vector was produced by PCR three rounds of PCR amplification using as a template a plasmid containing the cDNA of AMPKγ1, with a GOF mutation (R69Q) (a gift from Benoit Viollet, Institut Cochin, France). We used the following forward primers to add the c-Myc tag and Kozak sequence to AMPKγ1: RV69 5′-GGGGACAAGTTTGTACAA AAAAGCAGGCTGC CGCCACCATG-3′, RV70 5′-AAAGCAGGCTGCCGCCACCAT GGAAC AAAAACTTATTTCTGA AG-3′and RV71 5′-GAACAAAAACTTAT TTCTGAA GAAGATCTGATGGAGTCGGTTGCTGCAGAG-3′. We used as a reverse primer RV72 5′-GGGGACCACTTTGTACAA GAAAGCTGGGTATCAGGGCTTCTTCTCTCCTC-3′. The resulting product of the third round of PCR was cloned into pDONR221 by recombination *in vitro*, using the Gateway® Cloning technology following the protocol provided by the manufacturer (Life Technologies, Carlsbad, CA, USA). From the resulting entry vector, containing c-Myc-AMPKγ1GOF, we transferred this cDNA to both pcDNA3.1 (for cell transfection; see the Cell death assays section) and the SIN-cPPT-PGK-WHV Gateway vector (for *in vivo* manipulation of mouse brains; see the Injection of lentiviral vectors to the mouse brain section).

Mouse striatal cell culture

We used striatal cell lines expressing normal (7Q/7Q) or expanded (109Q/109Q) *Htt* derived from the HdhQ111 knock-in mice (30). These cells were handled as previously described (43) and, importantly, used at low passages (P9–P11).

Cell death assays

Cell death tests were performed as described previously inducing cell death by serum deprivation (71). Mouse striatal cells were seaded in 24-well plates. Cells were genetically manupulated using cDNAs (see the 'production of AMPKγ1GOF' section) or siRNAs (see below) or pharmacologically treated using metformin (1,1-dimethylbiguanide hydrochloride, Sigma-Aldrich ref. D150959) or vehicle (DMSO) for 24 h, prior to serum deprivation for an additional 24 h. Cells were fixed with PFA 4% and stained with 4′,6-diamidino-2-phenylindole (DAPI). Cells were then mounted on slides with polyvinyl alcohol. We examined dead cells each of which showed picnotic nuclei. Paired *t* tests were used for statistics.

Genetic perturbation in mouse striatal cells

cDNAs (2 µg) were transfected using JetPEI from PolyPlus Transfection (Illkirch, France) following the protocol of the manufacturer.

The siRNAs were transfected using JetSI-ENDO from PolyPlus Transfection (Illkirch, France) following the protocol of the manufacturer. The siRNAs were obtained from Eurofins MWG Operon (Ebersberg, Germany). The targeted sequences are as follows: AMPKα1_1, 5′-AACGAATTGAATGCTGTATAA; AMPKα1_2, 5′-AAATGGAAGGTTGGACGAAAA-3′; AMPKα2_1, 5′-AAAGTCA GAAGTGATGAATAG-3′; AMPKα2_2, 5′-AAATGGAAGGTT GGAC

GAAAA-3′. For pooled siRNA experiments, each siRNA was used at a concentration of 33 nM. Individual siRNAs were tested at 100 nM.

Real-time polymerase chain reaction

The relative expression of *Htt*, *Prkaa1* (mouse gene encoding AMPKα1) and *Prkaa2* (mouse gene encoding AMPKα2) was measured by RT-PCR using a thermal-cycler from Applied Biosystems (ViiATM 7 Real-Time PCR System; Life Technologies Corporation, Carlsbad, CA, USA) using the following TaqMan® gene expression assays: mm01213820_m1 for *Htt*, Mm012164789_m1 for *Prkaa1*, and Mm01296700_m1 for *Prkaa2*. We used for amplification the TaqMan® 2× PCR Master Mix from Applied Biosystems (Life Technologies Corporation). β2-microglobulin (β2m) gene (assay kit Mm00437762_m1) was used as a housekeeping gene. The RT-PCR program was as follows: 1 cycle of 2 min at 50°C, followed by 1 cycle of denaturation of 10 min at 95°C, continued by 40 cycles of 15 s of denaturation at 95°C and 60 s of annealing and polymerization at 60°C.

To detect polyQ expression in worms we used Taqman probes and primers from Integrated DNA Technologies (Coralville, IA, USA). The sequence of probe and primers to detect the housekeeping gene (*pmp-3*) are as follows: probe 5′-/56-FAM/TCC AGC AAG/ZEN/TTC TCC AAA ATC TCC AGT G/3IABkFQ/-3′, forward primer: 5′-AGG ACG ATC AGT TTC AAG GC-3′ and reverse primer: 5′-GTACCTCATCTACAGCTTCTC G-3′. For detection of the *GFP* gene we used: 5′-/56-FAM/ATAACCTTC/ZEN/GGGCATGGCACT CT/3IABkFQ/-3′, forward primer: 5′-CCTTCAAACTTGACTTCAG CAC-3′ and reverse primer: 5′-TGGTGTTCAATGCTTCTCGAG-3′. We used the same conditions and equipment described above.

Western blot analysis

Proteins from striatal cells were separated by sodium dodecyl sulphate–polyacrylamide gel electrophoresis (SDS–PAGE) and analysed by western blot using the following primary antibodies: mouse anti-htt (1HU-4C8, Millipore, 1:500), rabbit anti-AMPKα (23A3, Cell Signaling, 1:1000), and mouse anti-actin (MP, 1:10000). Secondary antibodies used: goat-anti-mouse IgG HRP-conjugated (Bio-Rad), goat-anti-rabbit IgG HRP-conjugated (Bio-Rad). Proteins were detected using ECL2 (ECL for actin) reagent (Pierce) and evaluated by densitometry and quantification was performed using ImageJ. For detection of AMPKα-phosphorylated, we used the rabbit anti-phospho-AMPKα (Thr172) (Cell Signaling, 1:1000). For detection of AMPKα1, we used the mouse anti-AMPKα1 antibody 2B7 (1:1000, Abcam). For detection of AMPKα2, we used the rabbit anti-AMPKα2 antibody ab3760 (1:500, Abcam). For detection of AMPKγ1 labelled with the c-Myc tag, we used the rabbit anti-Myc antibody 71D10 (1:1000, Cell Signaling).

Quantification of soluble mHtt levels in mouse striatal cells

Mutant Htt protein detection was performed as described previously (72). In brief, 5 µl lysate and 1 µl of antibody 2B7-Tb/MW1-D2 (73) per well were transferred to a low volume 384-well plate (Greiner). After incubation for 1 h under shaking wells, samples were analysed with an EnVision Reader (Perkin Elmer) following excitation at 320 nm (time delay 100 µs, window 400 µs, 100 flashes/well). Time-resolved fluorescence energy transfer signals were collected as the background subtracted ratio between fluorescence emission at 665 and 615 nm normalized to total protein content.

Confocal analysis in mouse striatal cells

Expression of AMPK subunits or phosphorylated AMPKα was analysed in 7Q/7Q and 109Q/109Q mouse striatal cells with or without metformin treatment (see the Cell death assays section) by using above-mentioned antibodies (see the Western blot analysis section). Mouse striatal cells were grown in a Nunc™ Lab-Tek™ 8-chamber Slide System (8000 cells/well). After 48 h, cells were fixed and permeabilized using Cytofix/Cytoperm™ kit (Becton, Dickinson and Company, Franklin Lakes, NJ, USA) following the manufacturer's protocol. Cells were then blocked with Dulbecco's phosphate buffered saline (DPBS) +0.1% Triton 100-X + 1% bovine serum albumin (BSA) for 1 h at room temperature and incubated overnight at 4°C with appropriate antibody (see above), at a dilution of 1:100 in DPBS 0.1% Triton 100-X and 1% BSA. The following day, cells were washed three times with DPBS for 10 min and incubated for 1 h and a half at room temperature with secondary antibodies goat-anti-mouse Alexa Fluor 488 (Invitrogen, 1:200) and goat-anti-rabbit Alexa Fluor 555 (Invitrogen, 1:200) for detection of AMPKα subunits or goat-anti-rabbit Alex Fluor 488 (Invitrogen, 1:200) for detection of phosphorylated AMPKα. Cells were then washed with DPBS and subjected to DAPI staining. After three more washes with DPBS, cells were mounted in Mowiol plus ProLong® Antifade Reagent (Life Technologies, Thermo Fisher Scientific). Fluorescent signals were quantified using an SP5 Leica Confocal Microscope (Leica Microsystems, Wetzlar, Germany). We kept the same settings in photomultipliers for each condition tested in order to ensure data comparability. Images were analysed using ImageJ. The comparison of 7Q/7Q and 109/109Q cells was based on cell nuclei that have a size of 150–250 pixels in each of the cell lines. To assess cytoplasmic expression of AMPKα isoforms, nuclear AMPK signals as defined by DAPI staining were blackened, and the remaining signals were quantified. To assess the nucleo-cytoplasmic distribution of AMPKα-phosphorylated, signals were quantified on either side of the nuclear membrane along a diameter line that crosses the cytoplasm and nucleus of each cell analysed. Statistical analysis was performed using *t* tests or ANOVA tests depending on the number of conditions compared in each genotype.

In vitro validation of c-Myc-AMPKγ1GOF plasmid expression

Of note, 293 T cells in six-well plates (750 000 cells/well) were transfected with 5 µg of plasmid and cultured for 72 h. Cellular lysates were harvested in a lysis buffer (20 mM Tris, pH 7.5, 2 mM ethylene glycol tetraacetic acid, 150 mM NaCl, 1% Nonidet P-40) containing protease inhibitors and phenylmethanesulfonyl fluoride (SIGMA, Saint Louis, USA). Protein concentrations were determined by the Bio-Rad protein assay kit (Bio-Rad, Munich, Germany). Equal amount of proteins were loaded on 10% SDS–PAGE and transferred to a nitrocellulose membrane (Schleicher and Scuell Bioscience GmbH, Dassel/Relliehausen, Germany). Immunoblotting was performed using a mouse monoclonal antibody (Ab-1, 1:200, Oncogene). Visualization of the protein was achieved using ECL (Amersham Biosciences Europe GmbH, Freiburg, Germany) in a Fusion FX system. The functionality of the vector was confirmed in 293 T cells transfected with SIN-cPPT-PGK-cMyc-AMPK-WHV where a strong signal corresponding to the expected molecular weight of cMyc-AMPKγ1 was detected.

Lentiviral vectors encoding the first 171 amino acids of mutated (82 CAG) Htt (Htt171-82Q), and a lentiviral vector encoding AMPKγ1, were produced as previously described (74,75). The

particle content of viral batches was determined with a p24 antigen enzyme-linked immunosorbent assay.

Injection of lentiviral vectors in the mouse brain

Thirteen adult 20 g male C57/BL6 mice were used (Iffa Credo/Charles River, Les Oncins, France). The animals were housed in a temperature-controlled room and maintained on a 12 h day/night cycle. Food and water were available *ad libitum*. The experiments were performed in accordance with the European Community directive (86/609/EEC) for the care and use of laboratory animals.

Concentrated viral stocks were thawed on ice and resuspended by repeated pipetting. The mice were anaesthetized using 75 mg/kg ketamine and 10 mg/kg xylazine, administered intraperitoneally. Lentiviral vectors were stereotaxically injected into the striatum using a 34-gauge blunt-tip needle linked to a Hamilton syringe (Hamilton, Reno, NV, USA) by a polyethylene catheter at the following stereotaxic coordinates: 0.5 mm rostral to bregma, 2 mm lateral to midline and 3.5 mm from the skull surface. Each mouse received the vector encoding mHtt alone in the left striatum and the vectors encoding both mHtt and AMPKγGOF in the right striatum.

Two hundred nanograms of p24 antigen of each viral vector was injected at 0.2 µl/min by means of an automatic injector (Stoelting Co., Wood Dale, USA) and the needle was left in place for an additional 5 min. The skin was closed using 4-0 Prolene suture (Ethicon, Johnson and Johnson, Brussels, Belgium).

Histological processing of mice brains

Seven weeks after lentiviral injection, animals received an overdose of sodium pentobarbital and were perfused transcardially with a phosphate-buffered saline solution followed by 4% paraformaldehyde (Fluka, Sigma, Buchs, Switzerland) and 10% picric acid fixation. Brains were removed and post-fixed in 4% paraformaldehyde and 10% picric acid for 24 h, and then cryoprotected in 30% sucrose, 0.1 M PBS for 48 h. A sledge microtome with a freezing stage at –25°C (SM2400; Leica Microsystems AG, Glattbrugg, Switzerland) was used to cut coronal brain sections of 25 µm thickness. Sections throughout the entire striatum were collected and stored free-floating in PBS supplemented with 0.12 µM sodium azide in 96-well plates at 4°C.

Striatal sections from injected mice were processed for immunohistochemistry for dopamine and cAMP-regulated phosphoprotein of a molecular mass of 32 kDa (DARPP-32, rabbit antibody SC11365, Santa Cruz Biotechnology, Santa Cruz, USA,) and ubiquitin (Ubi, rabbit antibody Z0458, Dakocytomation, Zug, Switzerland) following the same protocol. Sections were pre-incubated for 1 h in phenylhydrazin (107 251, Merck KGaA, Darmstadt, Germany) diluted at 1/1000 in PBS 0.1 M at 37°C. They were rinsed three times in PBS 0.1 M then incubated for 1 h in a blocking solution of 10% normal goat serum 0.1% Triton 100-X in PBS 0.1 M. Sections were incubated overnight at 4°C in a solution containing the first antibody diluted at 1/1000 (in the blocking solution for UBI, and in PBS 0.1 M 5% NGS for DARPP-32). They were then washed three times with PBS before applying the secondary antibody diluted at 1/200 in PBS-1%NGS (biotinylated goat anti-rabbit, BA1000; Vector Laboratories, Inc., CA, USA) for 1 h at room temperature. The complex was visualized using the Vectastain ABC kit (PK-6100, Vector Laboratories, West Grove, USA), with 3,3′-diaminobenzidine tetrahydrochloride (DAB metal concentrate; Pierce, Rockford, USA) as substrate. The sections were mounted, dehydrated by soaking twice in ethanol 100% and toluene solutions, and coverslipped with Eukitt (O. Kindler GmbH & CO, Freiburg, Germany).

Quantification of DARPP-32 lesions

The loss of DARPP-32 expression was analysed by collecting digitized images of ~12 sections per animal (150 µm between sections) with a slide scanner and by quantifying the lesion areas in square millimetre with an image analysis software (MCID Core 7.0, InterFocus Imaging, GE Healthcare Niagara, Inc., USA). Lesion areas in each section were determined as regions poor in DARPP-32 staining relative to the surrounding tissue. The volume was then estimated with the following formula: volume = $d \times (a1 + a2 + a3\cdots)$, where d is the distance between serial sections (25 µm), and $a1$, $a2$, $a3$ and on are DARPP-32-depleted areas for individual sections. The lesion size for each animal is expressed as the total lesion volume in 8–12 sections. The lesion volume for each group is expressed as mean ± SEM of individual mouse values. Statistical analysis was performed using a Wilcoxon test for paired samples (Statistica 5.1, Statsoft, Inc., USA). The significance level was set at $P < 0.05$.

Quantification of inclusion formation

For estimation of the number of UBI-positive mHtt inclusions, 12 coronal sections of the striatum (separated by 150 µm) were scanned with a 10× objective using a Zeiss Axioplan2 imaging microscope equipped with an automated motorized stage and acquisition system (Mercator Pro V6.50, ExploraNova). The quantification of all UBI-positive objects with an apparent cross-sectional area comprised between 1 and 50 µm² was performed as previously reported (76). The number of UBI-positive aggregates for each group is expressed as mean ± SEM of individual mouse values. Statistical analysis was performed using a Wilcoxon test for paired samples (Statistica 5.1, Statsoft, Inc., USA). The significance level was set at $P < 0.05$.

Supplementary Material

Supplementary Material is available at *HMG* online.

Authors' Contributions

C.N. conceived the experiments. R.P.V.M., F.F. and A.W. designed the experiments. R.P.V.M., F.F., K.C., M.D.S., J.A.P., J.M.M. and A.W. performed the experiments. R. P.V.M., F.F., K.C., M.D.S., J.A.P., J.M.M., A.W., N.D. and C.N. analysed and interpretated the data. R. P.V.M., N.D. and C.N. wrote the manuscript.

Acknowledgements

We thank H. Baylis, A. Fire, C. Ibañez-Ventoso, J. Xue, M. Driscoll and B. Viollet for gifts of plasmids, David Gems for non-*dyf sir-2.1*-overexpressing *C. elegans* mutants and the *Caenorhabditis* Genetic Centre for the provision of *C. elegans* strains. We also thank Nicolas Offner, Aurélie Darbois, Thomas Roux and Anne-Marie Orfila for technical assistance.

Conflict of Interest statement. None declared.

Funding

This study was supported by Agence Nationale de la Recherche (grants ANR-08-MNPS-0024-01 and ANR2012 BSV4 002302), France and by the Hereditary Disease Foundation and CHDI

Foundation, USA. R. P.V.M. had a Poste Vert fellowship from INSERM, France. R. P.V.M. is a 'Miguel Servet' fellow in Valencia (Ref.: CP11/00090), which is funded with a grant from the Instituto de Salud Carlos III (Madrid, Spain) which is partially supported by the European Regional Development Fund. This grant supported the work of R. P.V.M. and M.D.S. R. P.V.M. is also a Marie Curie fellow (CIG322034). Funding to pay the Open Access publication charges for this article was provided by ANR and the University Pierre and Marie Curie, France.

References

1. Carling, D. (2004) The AMP-activated protein kinase cascade—a unifying system for energy control. *Trends. Biochem. Sci.*, **29**, 18–24.
2. Carling, D., Thornton, C., Woods, A. and Sanders, M.J. (2012) AMP-activated protein kinase: new regulation, new roles? *Biochem. J.*, **445**, 11–27.
3. Viana, R., Aguado, C., Esteban, I., Moreno, D., Viollet, B., Knecht, E. and Sanz, P. (2008) Role of AMP-activated protein kinase in autophagy and proteasome function. *Biochem. Biophys. Res. Commun.*, **369**, 964–968.
4. Alers, S., Loffler, A.S., Wesselborg, S. and Stork, B. (2012) Role of AMPK-mTOR-Ulk1/2 in the regulation of autophagy: cross talk, shortcuts, and feedbacks. *Mol. Cell Biol.*, **32**, 2–11.
5. Chiacchiera, F. and Simone, C. (2010) The AMPK-FoxO3A axis as a target for cancer treatment. *Cell Cycle*, **9**, 1091–1096.
6. Mihaylova, M.M. and Shaw, R.J. (2011) The AMPK signalling pathway coordinates cell growth, autophagy and metabolism. *Nat. Cell. Biol.*, **13**, 1016–1023.
7. Shaw, R.J., Lamia, K.A., Vasquez, D., Koo, S.H., Bardeesy, N., Depinho, R.A., Montminy, M. and Cantley, L.C. (2005) The kinase LKB1 mediates glucose homeostasis in liver and therapeutic effects of metformin. *Science*, **310**, 1642–1646.
8. Canto, C. and Auwerx, J. (2009) PGC-1alpha, SIRT1 and AMPK, an energy sensing network that controls energy expenditure. *Curr. Opin. Lipidol.*, **20**, 98–105.
9. Egan, D.F., Shackelford, D.B., Mihaylova, M.M., Gelino, S., Kohnz, R.A., Mair, W., Vasquez, D.S., Joshi, A., Gwinn, D.M., Taylor, R. *et al.* (2011) Phosphorylation of ULK1 (hATG1) by AMP-activated protein kinase connects energy sensing to mitophagy. *Science*, **331**, 456–461.
10. Zhou, G., Myers, R., Li, Y., Chen, Y., Shen, X., Fenyk-Melody, J., Wu, M., Ventre, J., Doebber, T., Fujii, N. *et al.* (2001) Role of AMP-activated protein kinase in mechanism of metformin action. *J. Clin. Invest.*, **108**, 1167–1174.
11. He, H., Ke, R., Lin, H., Ying, Y., Liu, D. and Luo, Z. (2015) Metformin, an old drug, brings a new era to cancer therapy. *Cancer J.*, **21**, 70–74.
12. Nasri, H. and Rafieian-Kopaei, M. (2014) Metformin and diabetic kidney disease: a mini-review on recent findings. *Iran J. Pediatr.*, **24**, 565–568.
13. Apfeld, J., O'Connor, G., McDonagh, T., DiStefano, P.S. and Curtis, R. (2004) The AMP-activated protein kinase AAK-2 links energy levels and insulin-like signals to lifespan in *C. elegans*. *Genes Dev.*, **18**, 3004–3009.
14. Mair, W., Morantte, I., Rodrigues, A.P., Manning, G., Montminy, M., Shaw, R.J. and Dillin, A. (2011) Lifespan extension induced by AMPK and calcineurin is mediated by CRTC-1 and CREB. *Nature*, **470**, 404–408.
15. Salminen, A., Kaarniranta, K., Haapasalo, A., Soininen, H. and Hiltunen, M. (2011) AMP-activated protein kinase: a potential player in Alzheimer's disease. *J. Neurochem.*, **118**, 460–474.
16. Brown, K.A., Samarajeewa, N.U. and Simpson, E.R. (2013) Endocrine-related cancers and the role of AMPK. *Mol. Cell. Endocrinol.*, **366**, 170–179.
17. Steinberg, G.R. and Kemp, B.E. (2009) AMPK in health and disease. *Physiol. Rev.*, **89**, 1025–1078.
18. Zaha, V.G. and Young, L.H. (2012) AMP-activated protein kinase regulation and biological actions in the heart. *Circ. Res.*, **111**, 800–814.
19. Sarkaki, A., Farbood, Y., Badavi, M., Khalaj, L., Khodagholi, F. and Ashabi, G. (2015) Metformin improves anxiety-like behaviors through AMPK-dependent regulation of autophagy following transient forebrain ischemia. *Metab. Brain Dis.*, **30**, 1139–1150.
20. Ashabi, G., Khalaj, L., Khodagholi, F., Goudarzvand, M. and Sarkaki, A. (2015) Pre-treatment with metformin activates Nrf2 antioxidant pathways and inhibits inflammatory responses through induction of AMPK after transient global cerebral ischemia. *Metab. Brain Dis.*, **30**, 747–754.
21. Jiang, T., Yu, J.T., Zhu, X.C., Zhang, Q.Q., Tan, M.S., Cao, L., Wang, H.F., Shi, J.Q., Gao, L., Qin, H. *et al.* (2015) Ischemic preconditioning provides neuroprotection by induction of AMP-activated protein kinase-dependent autophagy in a rat model of ischemic stroke. *Mol. Neurobiol.*, **51**, 220–229.
22. Du, L.L., Chai, D.M., Zhao, L.N., Li, X.H., Zhang, F.C., Zhang, H. B., Liu, L.B., Wu, K., Liu, R., Wang, J.Z. *et al.* (2015) AMPK activation ameliorates Alzheimer's disease-like pathology and spatial memory impairment in a streptozotocin-induced Alzheimer's disease model in rats. *J. Alzheimers Dis.*, **43**, 775–784.
23. Lu, J., Wu, D.M., Zheng, Y.L., Hu, B., Zhang, Z.F., Shan, Q., Zheng, Z.H., Liu, C.M. and Wang, Y.J. (2010) Quercetin activates AMP-activated protein kinase by reducing PP2C expression protecting old mouse brain against high cholesterol-induced neurotoxicity. *J. Pathol.*, **222**, 199–212.
24. Ma, T., Chen, Y., Vingtdeux, V., Zhao, H., Viollet, B., Marambaud, P. and Klann, E. (2014) Inhibition of AMP-activated protein kinase signaling alleviates impairments in hippocampal synaptic plasticity induced by amyloid beta. *J. Neurosci.*, **34**, 12230–12238.
25. DiTacchio, K.A., Heinemann, S.F. and Dziewczapolski, G. (2015) Metformin treatment alters memory function in a mouse model of Alzheimer's disease. *J. Alzheimers Dis.*, **44**, 43–48.
26. Ma, T.C., Buescher, J.L., Oatis, B., Funk, J.A., Nash, A.J., Carrier, R.L. and Hoyt, K.R. (2007) Metformin therapy in a transgenic mouse model of Huntington's disease. *Neurosci. Lett.*, **411**, 98–103.
27. Ju, T.C., Chen, H.M., Lin, J.T., Chang, C.P., Chang, W.C., Kang, J. J., Sun, C.P., Tao, M.H., Tu, P.H., Chang, C. *et al.* (2011) Nuclear translocation of AMPK-alpha1 potentiates striatal neurodegeneration in Huntington's disease. *J. Cell Biol.*, **194**, 209–227.
28. Ju, T.C., Chen, H.M., Chen, Y.C., Chang, C.P., Chang, C. and Chern, Y. (2014) AMPK-alpha1 functions downstream of oxidative stress to mediate neuronal atrophy in Huntington's disease. *Biochim. Biophys. Acta.*, **1842**, 1668–1680.
29. Tourette, C., Farina, F., Vazquez-Manrique, R.P., Orfila, A.M., Voisin, J., Hernandez, S., Offner, N., Parker, J.A., Menet, S., Kim, J. *et al.* (2014) The Wnt receptor Ryk reduces neuronal and cell survival capacity by repressing FOXO activity during the early phases of mutant huntingtin pathogenicity. *PLoS Biol.*, **12**, e1001895.
30. Trettel, F., Rigamonti, D., Hilditch-Maguire, P., Wheeler, V. C., Sharp, A.H., Persichetti, F., Cattaneo, E. and MacDonald, M.E. (2000) Dominant phenotypes produced by the HD

mutation in STHdh(Q111) striatal cells. *Hum. Mol. Genet.*, **9**, 2799–2809.
31. Curtis, R., O'Connor, G. and DiStefano, P.S. (2006) Aging networks in *Caenorhabditis elegans*: AMP-activated protein kinase (aak-2) links multiple aging and metabolism pathways. *Aging Cell*, **5**, 119–126.
32. Lee, H., Cho, J.S., Lambacher, N., Lee, J., Lee, S.J., Lee, T.H., Gartner, A. and Koo, H.S. (2008) The *Caenorhabditis elegans* AMP-activated protein kinase AAK-2 is phosphorylated by LKB1 and is required for resistance to oxidative stress and for normal motility and foraging behavior. *J. Biol. Chem.*, **283**, 14988–14993.
33. Weimer, S., Priebs, J., Kuhlow, D., Groth, M., Priebe, S., Mansfeld, J., Merry, T.L., Dubuis, S., Laube, B., Pfeiffer, A.F. *et al.* (2014) D-Glucosamine supplementation extends life span of nematodes and of ageing mice. *Nat. Commun.*, **5**, 3563.
34. Lejeune, F.X., Mesrob, L., Parmentier, F., Bicep, C., Vazquez-Manrique, R.P., Parker, J.A., Vert, J.P., Tourette, C. and Neri, C. (2012) Large-scale functional RNAi screen in *C. elegans* identifies genes that regulate the dysfunction of mutant polyglutamine neurons. *BMC Genomics*, **13**, 91.
35. Owen, M.R., Doran, E. and Halestrap, A.P. (2000) Evidence that metformin exerts its anti-diabetic effects through inhibition of complex 1 of the mitochondrial respiratory chain. *Biochem. J.*, **348**(Pt 3), 607–614.
36. Parker, J.A., Arango, M., Abderrahmane, S., Lambert, E., Tourette, C., Catoire, H. and Neri, C. (2005) Resveratrol rescues mutant polyglutamine cytotoxicity in nematode and mammalian neurons. *Nat. Genet.*, **37**, 349–350.
37. Parker, J.A., Vazquez-Manrique, R.P., Tourette, C., Farina, F., Offner, N., Mukhopadhyay, A., Orfila, A.M., Darbois, A., Menet, S., Tissenbaum, H.A. *et al.* (2012) Integration of beta-catenin, sirtuin, and FOXO signaling protects from mutant huntingtin toxicity. *J. Neurosci.*, **32**, 12630–12640.
38. Greer, E.L., Oskoui, P.R., Banko, M.R., Maniar, J.M., Gygi, M.P., Gygi, S.P. and Brunet, A. (2007) The energy sensor AMP-activated protein kinase directly regulates the mammalian FOXO3 transcription factor. *J. Biol. Chem.*, **282**, 30107–30119.
39. Jeong, H., Cohen, D.E., Cui, L., Supinski, A., Savas, J.N., Mazzulli, J.R., Yates, J.R. III, Bordone, L., Guarente, L. and Krainc, D. (2012) Sirt1 mediates neuroprotection from mutant huntingtin by activation of the TORC1 and CREB transcriptional pathway. *Nat. Med.*, **18**, 159–165.
40. Jiang, M., Wang, J., Fu, J., Du, L., Jeong, H., West, T., Xiang, L., Peng, Q., Hou, Z., Cai, H. *et al.* (2012) Neuroprotective role of Sirt1 in mammalian models of Huntington's disease through activation of multiple Sirt1 targets. *Nat. Med.*, **18**, 153–158.
41. Park, S.J., Ahmad, F., Philp, A., Baar, K., Williams, T., Luo, H., Ke, H., Rehmann, H., Taussig, R., Brown, A.L. *et al.* (2012) Resveratrol ameliorates aging-related metabolic phenotypes by inhibiting cAMP phosphodiesterases. *Cell*, **148**, 421–433.
42. Burnett, C., Valentini, S., Cabreiro, F., Goss, M., Somogyvari, M., Piper, M.D., Hoddinott, M., Sutphin, G.L., Leko, V., McElwee, J.J. *et al.* (2011) Absence of effects of Sir2 overexpression on lifespan in *C. elegans* and *Drosophila*. *Nature*, **477**, 482–485.
43. Arango, M., Holbert, S., Zala, D., Brouillet, E., Pearson, J., Regulier, E., Thakur, A.K., Aebischer, P., Wetzel, R., Deglon, N. *et al.* (2006) CA150 expression delays striatal cell death in overexpression and knock-in conditions for mutant huntingtin neurotoxicity. *J. Neurosci.*, **26**, 4649–4659.
44. Salt, I., Celler, J.W., Hawley, S.A., Prescott, A., Woods, A., Carling, D. and Hardie, D.G. (1998) AMP-activated protein kinase: greater AMP dependence, and preferential nuclear localization, of complexes containing the alpha2 isoform. *Biochem. J.*, **334**(Pt 1), 177–187.
45. Inoki, K., Li, Y., Xu, T. and Guan, K.L. (2003) Rheb GTPase is a direct target of TSC2 GAP activity and regulates mTOR signaling. *Genes Dev.*, **17**, 1829–1834.
46. Sanchez, A.M., Csibi, A., Raibon, A., Cornille, K., Gay, S., Bernardi, H. and Candau, R. (2012) AMPK promotes skeletal muscle autophagy through activation of forkhead FoxO3a and interaction with Ulk1. *J. Cell Biochem.*, **113**, 695–710.
47. Baldo, B., Paganetti, P., Grueninger, S., Marcellin, D., Kaltenbach, L.S., Lo, D.C., Semmelroth, M., Zivanovic, A., Abramowski, D., Smith, D. *et al.* (2012) TR-FRET-based duplex immunoassay reveals an inverse correlation of soluble and aggregated mutant huntingtin in Huntington's disease. *Chem. Biol.*, **19**, 264–275.
48. Tabrizi, S.J., Scahill, R.I., Durr, A., Roos, R.A., Leavitt, B.R., Jones, R., Landwehrmeyer, G.B., Fox, N.C., Johnson, H., Hicks, S.L. *et al.* (2011) Biological and clinical changes in premanifest and early stage Huntington's disease in the TRACK-HD study: the 12-month longitudinal analysis. *Lancet Neurol.*, **10**, 31–42.
49. Neri, C. (2012) Role and therapeutic potential of the pro-longevity factor FOXO and its regulators in neurodegenerative disease. *Front Pharmacol.*, **3**, 15.
50. Kim, M., Lee, H.S., LaForet, G., McIntyre, C., Martin, E.J., Chang, P., Kim, T.W., Williams, M., Reddy, P.H., Tagle, D. *et al.* (1999) Mutant huntingtin expression in clonal striatal cells: dissociation of inclusion formation and neuronal survival by caspase inhibition. *J. Neurosci.*, **19**, 964–973.
51. Saudou, F., Finkbeiner, S., Devys, D. and Greenberg, M.E. (1998) Huntingtin acts in the nucleus to induce apoptosis but death does not correlate with the formation of intranuclear inclusions. *Cell*, **95**, 55–66.
52. Zala, D., Benchoua, A., Brouillet, E., Perrin, V., Gaillard, M.C., Zurn, A.D., Aebischer, P. and Deglon, N. (2005) Progressive and selective striatal degeneration in primary neuronal cultures using lentiviral vector coding for a mutant huntingtin fragment. *Neurobiol. Dis.*, **20**, 785–798.
53. Arrasate, M., Mitra, S., Schweitzer, E.S., Segal, M.R. and Finkbeiner, S. (2004) Inclusion body formation reduces levels of mutant huntingtin and the risk of neuronal death. *Nature*, **431**, 805–810.
54. Mitra, S., Tsvetkov, A.S. and Finkbeiner, S. (2009) Single neuron ubiquitin-proteasome dynamics accompanying inclusion body formation in Huntington disease. *J. Biol. Chem.*, **284**, 4398–4403.
55. Ben Sahra, I., Regazzetti, C., Robert, G., Laurent, K., Le Marchand-Brustel, Y., Auberger, P., Tanti, J.F., Giorgetti-Peraldi, S. and Bost, F. (2011) Metformin, independent of AMPK, induces mTOR inhibition and cell-cycle arrest through REDD1. *Cancer Res.*, **71**, 4366–4372.
56. Foretz, M., Hebrard, S., Leclerc, J., Zarrinpashneh, E., Soty, M., Mithieux, G., Sakamoto, K., Andreelli, F. and Viollet, B. (2010) Metformin inhibits hepatic gluconeogenesis in mice independently of the LKB1/AMPK pathway via a decrease in hepatic energy state. *J. Clin. Invest.*, **120**, 2355–2369.
57. Onken, B. and Driscoll, M. (2010) Metformin induces a dietary restriction-like state and the oxidative stress response to extend *C. elegans* Healthspan via AMPK, LKB1, and SKN-1. *PLoS One*, **5**, e8758.
58. Anisimov, V.N., Berstein, L.M., Popovich, I.G., Zabezhinski, M. A., Egormin, P.A., Piskunova, T.S., Semenchenko, A.V., Tyndyk, M.L., Yurova, M.N., Kovalenko, I.G. *et al.* (2011) If started early in life, metformin treatment increases life span and

postpones tumors in female SHR mice. *Aging (Albany NY)*, **3**, 148–157.
59. Cabreiro, F., Au, C., Leung, K.Y., Vergara-Irigaray, N., Cocheme, H.M., Noori, T., Weinkove, D., Schuster, E., Greene, N.D. and Gems, D. (2013) Metformin retards aging in *C. elegans* by altering microbial folate and methionine metabolism. *Cell*, **153**, 228–239.
60. Laberge, R.M., Sun, Y., Orjalo, A.V., Patil, C.K., Freund, A., Zhou, L., Curran, S.C., Davalos, A.R., Wilson-Edell, K.A., Liu, S. *et al.* (2015) MTOR regulates the pro-tumorigenic senescence-associated secretory phenotype by promoting IL1A translation. *Nat. Cell. Biol.*, **17**, 1049–1061.
61. Coughlan, K.S., Mitchem, M.R., Hogg, M.C. and Prehn, J.H. (2015) "Preconditioning" with latrepirdine, an adenosine 5′-monophosphate-activated protein kinase activator, delays amyotrophic lateral sclerosis progression in SOD1(G93A) mice. *Neurobiol. Aging*, **36**, 1140–1150.
62. Wong, V.K., Wu, A.G., Wang, J.R., Liu, L. and Law, B.Y. (2015) Neferine attenuates the protein level and toxicity of mutant huntingtin in PC-12 cells via induction of autophagy. *Molecules*, **20**, 3496–3514.
63. Wu, A.G., Wong, V.K., Xu, S.W., Chan, W.K., Ng, C.I., Liu, L. and Law, B.Y. (2013) Onjisaponin B derived from Radix Polygalae enhances autophagy and accelerates the degradation of mutant alpha-synuclein and huntingtin in PC-12 cells. *Int. J. Mol. Sci.*, **14**, 22618–22641.
64. Vingtdeux, V., Chandakkar, P., Zhao, H., d'Abramo, C., Davies, P. and Marambaud, P. (2011) Novel synthetic small-molecule activators of AMPK as enhancers of autophagy and amyloid-beta peptide degradation. *FASEB J.*, **25**, 219–231.
65. Brenner, S. (1974) The genetics of *Caenorhabditis elegans*. *Genetics*, **77**, 71–94.
66. Parker, J.A., Connolly, J.B., Wellington, C., Hayden, M., Dausset, J. and Neri, C. (2001) Expanded polyglutamines in *Caenorhabditis elegans* cause axonal abnormalities and severe dysfunction of PLM mechanosensory neurons without cell death. *Proc. Natl Acad. Sci. USA*, **98**, 13318–13323.
67. Lin, K., Dorman, J.B., Rodan, A. and Kenyon, C. (1997) daf-16: An HNF-3/forkhead family member that can function to double the life-span of *Caenorhabditis elegans*. *Science (New York)*, **278**, 1319–1322.
68. Tissenbaum, H.A. and Guarente, L. (2001) Increased dosage of a sir-2 gene extends lifespan in *Caenorhabditis elegans*. *Nature*, **410**, 227–230.
69. Walker, D.S., Vazquez-Manrique, R.P., Gower, N.J., Gregory, E., Schafer, W.R. and Baylis, H.A. (2009) Inositol 1,4,5-trisphosphate signalling regulates the avoidance response to nose touch in *Caenorhabditis elegans*. *PLoS Genet.*, **5**, e1000636.
70. Mello, C. and Fire, A. (1995) DNA transformation. *Methods Cell Biol.*, **48**, 451–482.
71. Gauthier, L.R., Charrin, B.C., Borrell-Pages, M., Dompierre, J.P., Rangone, H., Cordelieres, F.P., De Mey, J., MacDonald, M.E., Lessmann, V., Humbert, S. *et al.* (2004) Huntingtin controls neurotrophic support and survival of neurons by enhancing BDNF vesicular transport along microtubules. *Cell*, **118**, 127–138.
72. Weiss, A., Abramowski, D., Bibel, M., Bodner, R., Chopra, V., DiFiglia, M., Fox, J., Kegel, K., Klein, C., Grueninger, S. *et al.* (2009) Single-step detection of mutant huntingtin in animal and human tissues: a bioassay for Huntington's disease. *Anal. Biochem.*, **395**, 8–15.
73. Wild, E.J., Boggio, R., Langbehn, D., Robertson, N., Haider, S., Miller, J.R., Zetterberg, H., Leavitt, B.R., Kuhn, R., Tabrizi, S.J. *et al.* (2015) Quantification of mutant huntingtin protein in cerebrospinal fluid from Huntington's disease patients. *J. Clin. Invest.*, **125**, 1979–1986.
74. de Almeida, L.P., Ross, C.A., Zala, D., Aebischer, P. and Deglon, N. (2002) Lentiviral-mediated delivery of mutant huntingtin in the striatum of rats induces a selective neuropathology modulated by polyglutamine repeat size, huntingtin expression levels, and protein length. *J. Neurosci.*, **22**, 3473–3483.
75. Hottinger, A.F., Azzouz, M., Deglon, N., Aebischer, P. and Zurn, A.D. (2000) Complete and long-term rescue of lesioned adult motoneurons by lentiviral-mediated expression of glial cell line-derived neurotrophic factor in the facial nucleus. *J. Neurosci.*, **20**, 5587–5593.
76. Drouet, V., Perrin, V., Hassig, R., Dufour, N., Auregan, G., Alves, S., Bonvento, G., Brouillet, E., Luthi-Carter, R., Hantraye, P. *et al.* (2009) Sustained effects of nonallele-specific Huntingtin silencing. *Ann. Neurol.*, **65**, 276–285.